RELATIVE POSITIONING FOR UNDERWATER NAVIGATION OF MULTI-VEHICLE SYSTEMS

by

Göksel Berker Gönül

B.S., Mechanical Engineering, Boğaziçi University, 2021

Submitted to the Institute for Graduate Studies in
Science and Engineering in partial fulfillment of
the requirements for the degree of
Master of Science

Graduate Program in Mechanical Engineering
Boğaziçi University

2023

ACKNOWLEDGEMENTS

I sincerely would like to thank my thesis advisor, Assoc. Prof. Evren Samur, for his guidance, encouragement, and mentorship throughout my M.Sc. It would not have been possible without his support and motivation to complete this thesis.

I would also like to thank my former robotics team, BAUROV. Their generosity is admirable, not only for sharing their lab but also for their invaluable help.

I would especially like to thank the love of my life, Eda, for being a source of true happiness. You always being there for me gives me peace and confidence.

I would particularly like to thank Tolga Gürcan and Ahmet Kenan Gezici for their true friendship.

I would also like to express my gratitude to my thesis committee members for sparing their valuable time and for their reviews and corrections on my thesis.

Finally, I would like to express my thanks to my mother Havva Gönül, my father Muammer Gönül, and my dear sister Ezgi Gönül, who have always supported me and whom I am proud of.

ABSTRACT

RELATIVE POSITIONING FOR UNDERWATER NAVIGATION OF MULTI-VEHICLE SYSTEMS

Precise and accurate navigation is a significant problem for Autonomous Underwater Vehicle (AUV) applications. Due to limited electromagnetic penetration, GPS sensors are not an option for determining the position of an AUV. The most common method is called dead reckoning, which uses inertial measurement units (IMUs) with accelerometers and gyroscopes. Bias errors, misalignment and noisy measurements are common problems with IMUs. These errors make position information to be unreliable over long periods of time. Position errors grow rapidly due to velocity and angular random walk. The problem is further complicated when more than one vehicle is involved in a series of underwater tasks. Although conventional acoustic systems such as long baseline and ultra-short baseline have been developed to overcome the navigation problem, they are logistically complex and only cover a pre-deployed area. The process of deploying transponders and initialising them with precisely known locations makes the systems expensive and inappropriate for low cost AUVs. In order to eliminate growing errors of dead reckoning method, a system architecture with a navigation algorithm for N vehicles is proposed. This architecture makes use of a simple acoustic measurement system and a filtering algorithm. The simplicity of this acoustic measurements reduces the logistic complexities of conventional systems greatly. A leader-follower formation control is implemented, where there is a leader AUV and *N-1* follower AUVs. The system obtains relative positions between the leader and its followers, rather than absolute positions, to keep the formation intact. The follower AUVs position themselves according to the leader. This allows coordinated movements such as synchronised turns and manoeuvres without breaking the formation.

ÖZET

ÇOK ARAÇLI SİSTEMLERİN SU ALTI NAVİGASYONU İÇİN GÖRECELİ KONUMLANDIRMA

Bu tez çalışması, çoklu araçlı bir su altı ortamını incelemektedir. Hassas ve doğru navigasyon, Otonom Su Altı Aracı(AUV) uygulamaları için önemli bir problemdir. Sınırlı elektromanyetik penetrasyon nedeniyle, küresel konumlandırma sensörleri bir AUV'nin konumunu belirlemek için bir seçenek değildir. En yaygın yöntem, ivme ölçerler ve jiroskoplar içeren ataletsel ölçüm birimlerini (IMU) kullanan parakete seyir hesabı olarak adlandırılır. IMU'larla yanıltma hataları, hizalama hataları ve gürültülü ölçümler yaygın problemlerdir. Bu hatalar, pozisyon bilgisinin uzun süreli olarak güvenilmez olmasına neden olur. Pozisyon hataları hız ve açısal rastgele yürüyüş nedeniyle hızla büyür. Birden fazla aracın bir dizi su altı görevinde yer aldığı durumlar daha da karmaşıktır. Uzun Baz Hattı (LBL) ve Ultra-Kısa Baz Hattı (USBL) gibi geleneksel akustik sistemler, navigasyon sorununu aşmak için geliştirilmiştir, ancak lojistik olarak karmaşıktır ve yalnızca önceden kuruldukları alana özgü çalışırlar. Ses kaynaklarının yerleştirilmesi ve kesin olarak bilinen konumlarla başlatılması süreci, sistemlerin maliyetini artırdığından ve düşük maliyetli AUV'ler için uygun olmayan hale getirir. Bu makale, *N* araç için bir navigasyon algoritmasıyla bir sistem mimarisi önermektedir. Bir lider AUV ve *N-1* takipçi AUV'lerin bulunduğu bir lider-takipçi formasyon kontrolü uygulanır. Sistem, formasyonu korumak için lider ve takipçileri arasındaki göreceli konumları, mutlak konumlar yerine kullanır. Takipçi AUV'ler liderin hareketlerine göre konumlarını alırlar. Bu sistem, formasyonu bozmadan senkronize dönüşler ve manevralar gibi koordineli hareketlere olanak sağlar.

TABLE OF CONTENTS

LIST OF FIGURES

LIST OF TABLES

LIST OF SYMBOLS

A	State Transition Matrix
$a_{x,y,z}$	Acceleration at Earth-Fixed Frame
$a^b_{x,y,z}$	Acceleration at Body-Fixed Frame
B	State Input Matrix
dt	Time Step
$F_{x,y,z}$	Force Vector Components
G	State Noise Matrix
H	Observation Matrix
$M_{x,y,z}$	Moment Vector Components
P_k	State Error Covariance Matrix at k^{th} step
$\widehat{P}_k$	State Error Covariance Prediction Matrix at k^{th} step
Q	State Noise Covariance Matrix
R	Measurement Noise Covariance Matrix
r	Range Measurement
u_k	Input Vector at k^{th} step
v_k	Noise Vector at k^{th} step
x_k	State Vector at k^{th} step
$\widehat{x}_k$	State Prediction Vector at k^{th} step
z	Measurement Vector
β	Sonar Angle
θ	Pitch Angle
ρ	Variance Gain
σ	Variance
ϕ	Roll Angle
ψ	Yaw Angle

LIST OF ACRONYMS/ABBREVIATIONS

2D	Two Dimensional
3D	Three Dimensional
AUV	Autonomous Underwater Vehicles
CN	Cooperative Navigation
CNA	Communication and Navigation Aids
DR	Dead Reckoning
DVL	Doppler Velocity Log
EKF	Extended Kalman Filter
EMW	Electromagnetic Wave
GPS	Global Positioning System
IMU	Inertial Measurement Units
INS	Inertial Navigation System
LBL	Long Base Line
LIDAR	Light Detection and Ranging
RN	Relative Navigation
SINS	Strapdown Inertial Navigation System
ToA	Time of Arrival
ToAD	Time of Arrival Difference
USBL	Ultra Short Base Line
VD	Vehicle Dynamics

1. INTRODUCTION

1.1. Background

Accurate navigation is essential for any robot. It becomes even more complex when operating in a challenging medium such as underwater. In recent years, research into Autonomous Underwater Vehicles (AUVs) has increased significantly. Accurate navigation of an AUV improves the capabilities of the vehicle [1]. The performance of the navigation algorithm depends on both the sensor measurements and the vehicle model. The accuracy of the measurements can be increased with the quality of the individual sensors, which results in higher costs. Much research is being done to develop novel algorithms to improve the quality of the measurements without changing the sensors used.

Although it is well known that the use of different types of sensors can improve navigation performance, the options are limited when working with AUVs. Most robotic applications obtain absolute positions from Global Navigation Satellite Systems or Global Positioning System (GPS). However, these are not possible for underwater applications due to the strong attenuation of electromagnetic waves in aquatic environments [2]. Only a limited number of underwater robots are equipped with GPS sensors, and they are often required to come to the surface to obtain a position fix signal and then return to the water.

Another sensor type that is not applicable is light detection-based sensors. The most common of these is the Light Detection and Ranging (LIDAR) sensor. There are many simultaneous localization and mapping algorithms that benefit from LIDAR sensors to create a map by measuring the distance of the surroundings using the Time of Arrival (ToA) of reflected beams. Since the penetration depth of the infrared electromagnetic waves (EMV) in water is less than 10 meters as seen from Table 1.1 [3], it is impossible to use LIDAR sensors, that operate in the infrared spectrum commercially.

Table 1.1. Electromagnetic penetration depth of EMV according to their wavelength spectrum [3].

EMV Type	**Penetration Depth Level (1/e)**
Ultraviolet	10^{-6} - 10^{5} mm
Visible	10^{5} - 10^{1} mm
Infrared	10^{1} - 10^{-2} mm
Microwave	10^{-2} - 10^{1} mm

Acoustic navigation and inertial navigation are the most preferred methods for implementation in an underwater robot [4]. Many studies benefit from sending and receiving sound waves and calculating position/orientation by measuring the phase shift of the acoustic waves, the Time of Arrival (ToA) and the Time of Arrival Difference (ToAD). Absolute positions are obtained using acoustic systems such as Long Base Line (LBL). While LBL is widely used, deploying many transponders on the seafloor and initializing them with the precise positions is costly and difficult to implement [5]. To overcome this problem, Ultra Short Base Line (USBL) with a single transponder can be used [6]. A common USBL system makes use of a transceiver mounted on a pole under a ship to communicate with a responder mounted on the AUV.

In order to provide accurate motion detection, underwater vehicles today use commercially available Inertial Measurement Units (IMU) [7]. Conventional inertial navigation systems (INS) that use IMUs measure the vehicle's velocity with accelerometers and its attitude angle with gyroscopes [8]. Acceleration and angular velocity measurements in IMUs are high frequency but quite noisy. Velocities, positions and orientations are obtained by integrating the measurements from the IMU. Due to the integration of noise terms, positions and orientations start to drift with a random walk. Errors increase over time.

Even though researchers has developed various methods and applications to improve the navigation accuracy of INS, it is not possible to eliminate a typical random error of gyroscopes and accelerometers by conventional calibration and compensation

procedures [9]. The basic solution is to enhance the precision of sensor manufacture. This requires more advanced materials and devices which are costly and time consuming to achieve. Even the random error is white and Gaussian, an integration of the noise causes random walk process. It means that random error is added at each step. The total error becomes cumulative and the measured value deviates from the true value.

While IMUs perform well over short periods of time, they do not provide global position measurements. Relying on INS alone results in cumulative navigational drift [10]. Dead Reckoning (DR) is an INS-based navigation technique that sums position displacements from a known position. The displacement estimates can be in the form of changes in Cartesian coordinates or in heading angle and distance. The increasing position errors of DR can be kept within predefined limits, but it requires sufficiently frequent absolute position updates [11].

The multi-robot AUV environment is of interest because a single-robot approach suffers from the fact that the failure of a single robotic unit can prevent the success of the whole task. However, due to the versatility of its multiple agents, the multi-robot or swarm approach can take advantage of parallelism to be more efficient. [12]. In the recent past, many researchers have developed multi-agent methods for formation control, but most methods are not directly applicable to an underwater environment [13]. The most widely used method is the leader-follower approach because of its simplicity and ease of extension [14]. The leader follows the path in a predetermined trajectory and the followers move according to the leader to maintain the desired formation structure. Formation control is achieved by changing the trajectory of the leader and aligning the followers to maintain the structure.

1.2. Motivation

An accurate navigation system is needed for multi-robot underwater applications because applicable sensor types are limited. Acoustic solutions such as LBL systems

are challenging and expensive to deploy. The deployment configuration is specific to a mission since they cover a limited geographic area. Hence, they do not offer a better solution for cost efficient AUVs. Also, the dead reckoning approach may not be useful for small and low-cost AUVs for long durations in a mission. Random walks of velocity and angle causes the position and orientation error of each vehicle to become larger. In addition, eliminating deterministic errors makes IMUs expensive and large in dimensions. Table 1.2 [15] shows the cost of IMUs according to their error levels.

Table 1.2. Cost of IMU according to their class [15].

	Tactical Grade	**Navigation Grade**	**Strategic Grade**
Gyroscope Drift	1-10 deg/h	0.015 deg/h	0.0001 deg/h
Acceleration Bias	100 - 1000 μg	50 - 100 μg	1 μg
Cost	<10000 $	10000 – 70000 $	> 200000 $

Although the existing acoustic and inertial solutions are extensively used nowadays, there is still a vast room for improvement. Much research is conducted to increase the measurement quality without increasing the cost. Therefore, the development of novel algorithms to enhance the measurement quality without changing the hardware has been a topic of interest in recent years. A low cost system architecture that provides an accurate navigation for the promising field of multi-robot underwater environments is needed.

The objective of the research is to observe whether a Kalman filter based navigation algorithm can be used to improve the relative positions of two distinct vehicles. The expected outcome is that, an optimal estimation that eliminates random walks and noisy measurements can be designed for a multi-robot underwater environment.

The goal is to design a navigation algorithm to be used in underwater swarm applications. The system is constructed with the aims in the following :

(i) Establishing an acoustic navigation system that is able to measure relative position between two underwater vehicles and,
(ii) developing a navigation algorithm for the follower AUV to keep its relative position to the leader AUV steady.

2. LITERATURE REVIEW

Underwater navigation is popular among the researchers since it is a complex problem and there is a lot of room for improvement. There are several approaches to this problem such as acoustic-based, vision-based and statistical-based. Each approach has its own limitations and advantages.

The strapdown inertial navigation system (SDINS) is used in most of robotic applications from aviation to underwater. SDINS provides measurements of linear accelerations and angular rates through its accelerometers and gyroscopes aligned along three orthogonal axes [16]. Even though the SDINS is accurate in the short term, the position, velocity and angular orientation errors increase unboundedly due to deterministic errors, stochastic errors and sensor imperfections [17]. To limit these errors, commonly some auxiliary sensors are integrated with the SDINS. In an integrated underwater navigation system, the auxiliary sensors typically consist of a Doppler Velocity Log (DVL), an inclinometer, a depthmeter, and a gyrocompass [1]. Typical auxiliary sensors are listed in the Table 2.1 [18].

Table 2.1. Auxiliary sensors for underwater navigation applications [18].

SENSOR	**VARIABLE**	**PRECISION**	**RANGE**
Altimeter	Altitude	0.01-1.0 m	varies
Inclinometer	Roll, Pitch	$0.1^o - 1^o$	+/- 45^o
Pressure	Depth	1 % - 0.01%	full ocean depth
Compass	Heading	$1 - 10^o$	360^o
12 kHz LBL	XYZ Position	0.1-10 m	5-10 km
300 kHz LBL	XYZ Position	+/- 0.007 m	100 m
DVL	v_{body}	0.3% or less	18 - 100 m
GPS	XYZ Position	0.1-10 m in air	In water: 0 m

According to Morgado et al., a navigation system is proposed specifically for an AUV, named Infante [19]. The dynamics of the vehicle is introduced to the navigation system, which includes auxiliary sensors and INS [19]. An acoustic aided navigation is constructed with a USBL sensor that gets position updates. A simplified flowchart is illustrated in Figure 2.1 [19].

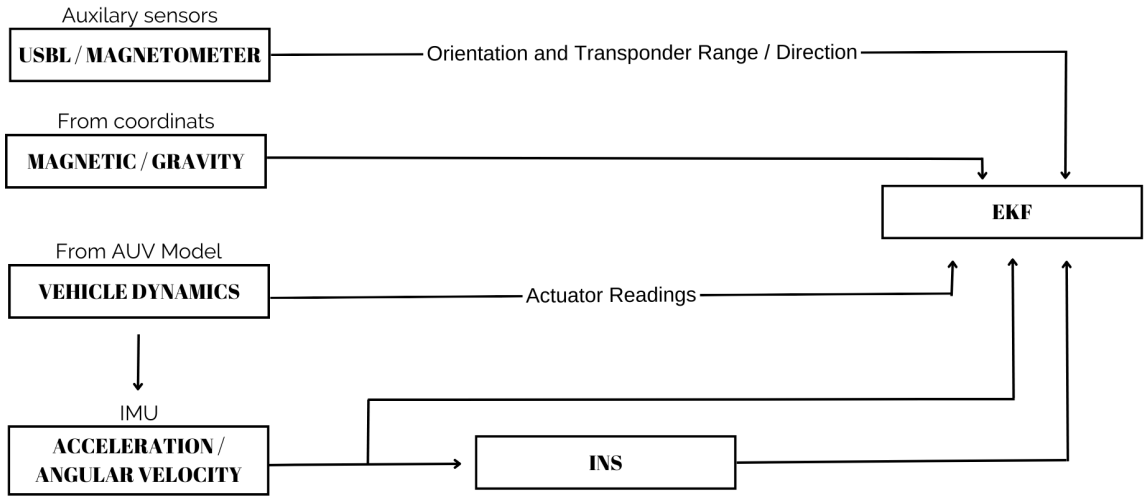

Figure 2.1. Proposed navigation system by Morgado et al. [19].

Lee et al. proposed an estimation for an AUV's trajectory by obtaining range measurements from a single transponder [7]. The transponder is placed in a known location and the AUV measures the distance from the transponder using acoustic beams shown in Figure 2.2. The auxiliary sensors are magnetometers that provide heading and pitch measurements. There are two main assumptions in the paper by Lee et al. First, the vehicle is cruising at a constant speed. Second, the vehicle is not at the same depth as the transponder in order to keep the observability matrix at full rank. The kinematic model of the vehicle in polar coordinates is used for the prediction step. The measurements from the acoustic transponder and the magnetometers are fused with the estimation of an Extended Kalman Filter. The simulation results show that the position error does not exceed two meters in root mean square [20].

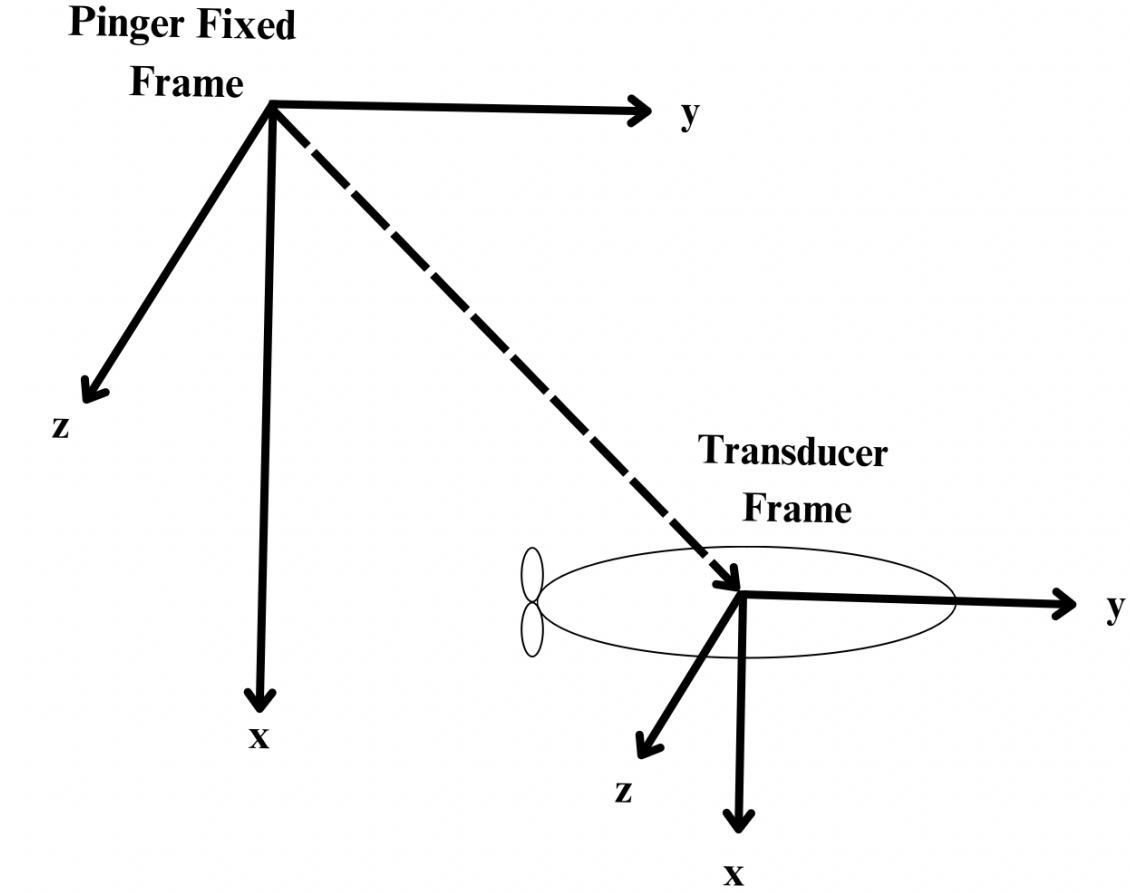

Figure 2.2. Acoustic beams from a single transponder on an AUV [7].

Bahr et al. suggested a navigation system architecture for multiple AUVs [21]. The research presents an algorithm for Cooperative Navigation (CN) for two types of vehicles [21]. The first type is Communication and Navigation Aids (CNA). CNAs are equipped with more expensive and accurate navigation suite. They can operate in shallow water and/or on the surface to receive the GPS signal for a bounded error. The second type is AUVs, which perform an underwater mission with a much simpler and cheaper navigation equipment. The CNAs serve as moving beacons for the AUVs while they perform missions. In the system all vehicles broadcast their positions and receive range measurements via their acoustic modems. The research by Bahr et al. comes with two main assumptions [21]. First one is that information exchange between vehicles are possible. Secondly, range measurements from acoustic signals can be performed. An AUV predict their own state through their DR sensors. If it receive a signal from another AUv and/or CNA, an algorithm is run to update their position. Four separate

algorithms are developed for unique cases. Each of the algorithms is described below:

- Algorithm 1 is applied for when CNA receives a signal from an AUV.
- Algorithm 2 is applied for when CNA receives a signal from an CNA.
- Algorithm 3 is to determine the time for CNA when to broadcast.
- Algorithm 4 is to determine the optimal position for CNA.

Fan et al. gives a comprehensive study about Terrain-Aided Navigation (TAN) [22]. TAN provides an auxiliary measurements to an AUV to navigate itself. TAN method relies on feature extraction and object matching. The AUV either detects a landmark or a geologic structure and uses a matching algorithm to obtain position measurement [22]. If the object that is detected by an AUV is at a known location, the AUV can locate itself on a map where the object is placed. Another way to perform TAN is to map sea bottom. If the bathymetry information is known, the AUV can match the measured sea floor and locate itself as well.

Many researchers are still developing novel sensor integrations or algorithms to overcome the underwater navigation problem. Acoustic solutions and auxiliary sensors seem to improve performance significantly, but these solutions come with higher costs and/or logistical complexities. Improving sensor manufacturing is another option, but it is expensive and time consuming. There is still a lot of room for development to improve underwater navigation.

3. MATERIALS AND METHODS

3.1. System Overview

This section introduces a simple and easily implementable acoustic navigation system architecture and a Kalman-based algorithm for a multi-robot underwater environment. The system to be analyzed consists of *N* number of AUVs where there is a leader and *N-1* followers. Accurate positioning is required for coordinated navigation, where the vehicles navigate while maintaining their formation. Instead of obtaining absolute positions in an earth fixed frame, as is common practice, the proposed method uses relative positioning where the followers continuously position themselves according to the leader. Relative positioning is illustrated in Figure 3.1.

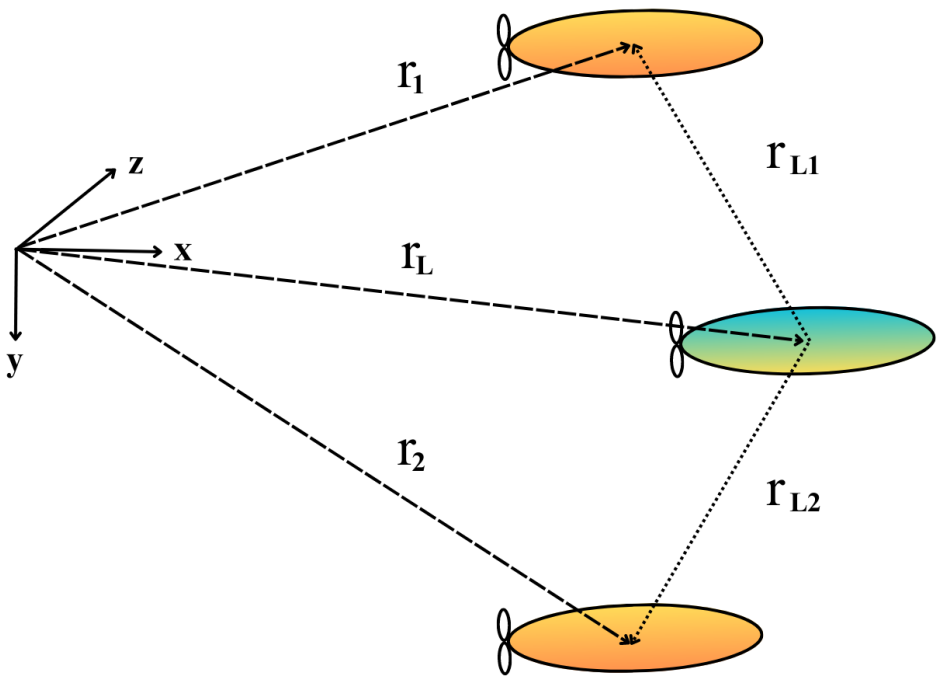

Figure 3.1. Relative navigation representation where two follower AUVs has relative distances to a leader represented by green color [23].

The reliability of the navigation is critical in the leader-follower approach to maintain the structure and avoid collisions between followers. In most applications, relative positioning is sufficient for the followers to adjust their course if there is a deviation on the leader's path or if the leader changes course.

The following assumptions are made for this study. The leader and follower AUVs are equipped with IMU sensors that provide accelerations in three axes as output. The leader AUV is also fitted with an acoustic transponder that produces sound waves at a specific frequency. The leader AUV moves along a predefined path. The follower AUVs are also equipped with IMU sensors that provide acceleration measurements in three axes. They have at least three transducers that receive the sound wave generated by a pinger on the leader AUV. The assumptions in this study are detailed below.

- Each AUV has an IMU that provides acceleration measurements in three earth-fixed axes with zero mean white Gaussian noise.
- The leader has a transponder that generates sound waves.
- The followers have at least three transducers that receive sound waves.
- The leader and followers are close enough that wave attenuation is negligible.
- The leader sends its own IMU data to the followers by an acoustic communication.
- The initialization is synchronised.

Transducer-transponder pairs are used to transmit and receive sound waves. In many applications they are used for range and angle measurements by ToA and ToAD calculations. In the proposed system, the relative position between the leader and a follower is obtained by the trilateration method as shown in Figure 3.2 [24].

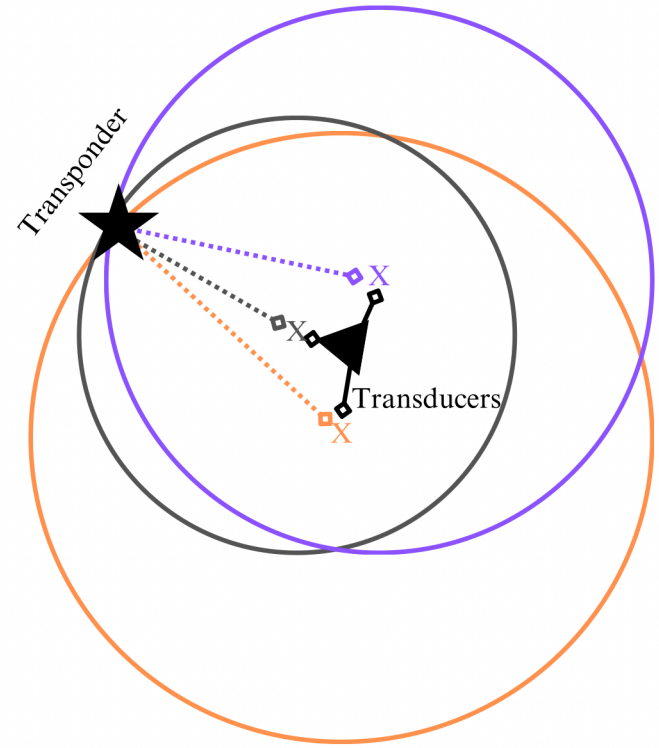

Figure 3.2. Trilateration with three distinct points [24].

When a transponder generates a sound wave, the transducers will receive the wave and calculate the distance to the transponder using the speed of sound under water and the ToA. A minimum of three separate transducers are required to perform trilateration. After the calculation, the follower knows the relative distance to the leader in all three axes. This measurement and its derivative provide an update of the absolute relative position or relative velocity between the vehicles.

3.2. Kalman Algorithm

Estimating the state underlies all navigating algorithms [25]. The Kalman filter is a method to obtain an optimal recursive estimation of a dynamic system. Although it is based on the results of complex computations of probability theory, its final formulation is surprisingly simple and effective to implement on a processor [26].

The Kalman algorithm consists of two steps, prediction and updating. This study introduces a Kalman based algorithm that utilizes prediction and update parts recursively. The prediction state is to give an estimation about how the states are going to change considering dynamics and the environmental effects. The update part of the algorithm improves this estimation by fusing the measurements coming from the sensors.

3.2.1. Prediction

From the k^{th} step, the $k+1^{th}$ step is obtained by the state transition matrix and the inputs. A linear stochastic process for a discrete-time-finite-dimensional system can be defined as:

$$\widehat{x}_k = Ax_k + Bu_k + Gv_k, \tag{3.1}$$

$$\widehat{P}_k = AP_kA^T + Q, \tag{3.2}$$

where x_k is the state vector, A is the state transition vector and u_k, v_k are the deterministic process input and process noise respectively. Here the matrix Q is the process covariance matrix that corresponds to the process noise.

3.2.2. Updating

The Kalman gain is calculated and the state prediction is updated with a new measurement. According to the Kalman Gain, a new state estimation is calculated and the state covariance matrix P_{k+1} is updated as:

$$K = (\widehat{P}_kH)(H\widehat{P}_kH^T + R)^{-1}, \tag{3.3}$$

$$x_{k+1} = \widehat{x}_k + K(z_k + H\widehat{x}_k), \tag{3.4}$$

$$P_{k+1} = (I - KH)\widehat{P}_k. \tag{3.5}$$

The matrix R is the measurement covariance matrix, z is the measurement vector and K is the Kalman gain. The states are the relative positions, velocities and accelerations between the leader and a follower. The kinematic model can be applied to the state transition matrix. When Equation (3.1) is applied to the proposed system, the

kinematic discrete-time state prediction matrix for the relative position of a follower in 2D is constructed as:

$$\begin{bmatrix} \widehat{x}_{rel} \\ \widehat{\dot{x}}_{rel} \\ \widehat{\ddot{x}}_{rel} \\ \widehat{y}_{rel} \\ \widehat{\dot{y}}_{rel} \\ \widehat{\ddot{y}}_{rel} \end{bmatrix}_k = \begin{bmatrix} 1 & dt & dt^2/2 & 0 & 0 & 0 \\ 0 & 1 & dt & 0 & 0 & 0 \\ 0 & 0 & 1 & 0 & 0 & 0 \\ 0 & 0 & 0 & 1 & dt & dt^2/2 \\ 0 & 0 & 0 & 0 & 1 & dt \\ 0 & 0 & 0 & 0 & 0 & 1 \end{bmatrix} \begin{bmatrix} x_{rel} \\ \dot{x}_{rel} \\ \ddot{x}_{rel} \\ y_{rel} \\ \dot{y}_{rel} \\ \ddot{y}_{rel} \end{bmatrix}_k . \tag{3.6}$$

The state is predicted from the states of the k^{th} step. This means that an estimate of how the relative states between the leader and a follower will change is proposed using kinematic equations with no deterministic input Bu_k. The prediction of the matrix P is based on the process noise denoted by Q. The matrix Q is obtained with the Discrete Wiener Process Acceleration (DWPA) model as:

$$Q_k = \rho_k \sigma^2 \rho_k^T, \tag{3.7}$$

$$\rho_k = \begin{bmatrix} dt^2/2 \\ dt \\ 1 \end{bmatrix}. \tag{3.8}$$

DWPA models the effects of the linear acceleration process noise on velocity and position estimations. It shows the integrated noise effects on the states. The noise variance should be multiplied by the noise gain to construct the Q matrix. The gain is denoted by ρ and the noise variance is denoted by σ in the Equations (3.7) and (3.8) [27].

The measurement matrix z is constructed from acoustic and IMU measurements. The relative positions and velocities are obtained from the acoustic measurements. The relative acceleration measurement is obtained by the difference of the IMU measurements of the leader and the follower. The accelerometers on AUV provide outputs much more frequently than the acoustic sensors in the system. The Kalman filter algorithm

is computed at the frequency of the accelerometers and the acoustic measurements are assumed to be constant until a new measurement is obtained for the algorithm. The measurement matrix z is obtained from the sensor measurements as such:

$$\begin{bmatrix} x_{rel} \\ \dot{x}_{rel} \\ \ddot{x}_{rel} \\ y_{rel} \\ \dot{y}_{rel} \\ \ddot{y}_{rel} \end{bmatrix}_{measurement} = \begin{bmatrix} 1 & 0 & 0 & 0 & 0 & 0 \\ 0 & 1 & 0 & 0 & 0 & 0 \\ 0 & 0 & 1 & 0 & 0 & 0 \\ 0 & 0 & 0 & 1 & 0 & 0 \\ 0 & 0 & 0 & 0 & 1 & 0 \\ 0 & 0 & 0 & 0 & 0 & 1 \end{bmatrix} \begin{bmatrix} x_{acoustic} \\ \dot{x}_{acoustic} \\ \ddot{x}_{l_{imu}} - \ddot{x}_{f_{imu}} \\ y_{acoustic} \\ \dot{y}_{acoustic} \\ \ddot{y}_{l_{imu}} - \ddot{y}_{f_{imu}} \end{bmatrix}. \tag{3.9}$$

The relative positions in Equation (3.9), $x_{acoustic}$ and $y_{acoustic}$, are directly obtained from acoustic measurements. The relative velocities, $\dot{x}_{acoustic}$ and $\dot{x}_{acoustic}$, are derived by taking derivatives of the relative positions. Lastly, the relative accelerations $\ddot{x}_{rel}$ and $\ddot{y}_{rel}$, are obtained from the IMUs.

The covariance matrix R is obtained from the sensor noise. Since each measurement is independent of the others, the matrix R can be modelled as a diagonal matrix where each term is the variance of the noise measurements. The Equations (3.3), (3.4) and (3.5) are computed to obtain the $k + 1^{th}$ step of the state. The algorithm is run recursively for each follower AUV to achieve an accurate navigation.

3.3. Simulation

Two or more vehicles can be spawned in the MATLAB/Simulink environment and the sensor models and associated measurements can be generated. REMUS-100 is an open-source AUV that takes its name from its maximum operating depth of 100 meters. It was developed by the Woods Hole Oceanographic Institution (WHOI) [28]. REMUS-100 has a propeller that generates longitudinal thrust at the rear. It has moving blades that allow to control of the rotational motion. Several controller designs for the REMUS-100 AUV can be found in the literature. PD controller is implemented for the depth control of REMUS [29]. PID controller is available to control the yaw

rate of REMUS [30]. REMUS vehicle is useful to implement in simulation environment to make test runs for evaluating a navigation model.

The REMUS vehicle is vastly used for research purposes because its dynamics are well-known. Hydrodynamic model of the REMUS is already studied several times. Generally, obtaining hydrodynamic coefficients of a vehicle requires expensive tests and trials. Since REMUS is popular among researchers, its hydrodynamic model is available. Even though its shape is not similar with the AUV used in experimental trials, it is used in simulation environment. The main reason of this selection is the availability of the hydrodynamic model and the desire of testing the proposed system with a real vehicle model.

Dynamics of the REMUS in the simulation are based on rigid body kinetics. Forces and the moments applied to the AUV are composed of hydrostatic forces, hydrodynamic forces and gravitational forces. Hydrostatic effects result in buoyancy. Hydrodynamic effects can be in form of drag forces, lift forces and added mass effect. All these forces and moments can be summarized as [29]:

$$F_x = X_{HS} + X_{u|u|}u|u| + X_{wq}wq + X_{qq}qq + X_{vr}vr + X_{rr}rr, \tag{3.10}$$

$$F_y = Y_{HS} + Y_{v|v|}v|v| + Y_{r|r|}r|r| + Y_{ur}ur + Y_{wp}wp + Y_{pq}pq + Y_{uv}uv, \tag{3.11}$$

$$F_z = Z_{HS} + Z_{w|w|}w|w| + Z_{q|q|}q|q| + Z_{uq}uq + Z_{vp}vp + Z_{rp}rp + Z_{uw}uw, \tag{3.12}$$

$$M_x = K_{HS} + K_{p|p|}p|p|, \tag{3.13}$$

$$M_y = M_{HS} + M_{w|w|}w|w| + M_{q|q|}q|q| + M_{uq}uq + M_{vp}vp + M_{rp}rp + M_{uw}uw, \tag{3.14}$$

$$M_z = N_{HS} + N_{v|v|}v|v| + N_{r|r|}r|r| + N_{ur}ur + N_{wp}wp + N_{pq}pq + N_{uv}uv. \tag{3.15}$$

The first three equations above represent linear translational motion. F represents forces, M represent moments. u, v, w are the velocities in the body-fixed frame. p, q, r represent rotational velocities along three axes. HS subscript is used to denote hydrostatic force and moment components. The coefficients are defined in Table A1.1 and Table A1.2.

When A is constructed, added mass is implemented with $X_{\dot{u}}$, $Y_{\dot{v}}$, $Y_{\dot{r}}$, $Z_{\dot{w}}$, $Z_{\dot{q}}$ terms. These coefficients can be found in Table A1.3. x_g, y_g, z_g are the locations of center of gravity defined in body-fixed coordinates. The derivative of the state vector can be found by Equation (3.17),

$$A = \begin{bmatrix} m - X_{\dot{u}} & 0 & 0 & 0 & mz_g & -my_g \\ 0 & m - Y_{\dot{v}} & 0 & -mz_g & 0 & mx_g - Y_{\dot{r}} \\ 0 & 0 & m - Z_{\dot{w}} & my_g & -mx_g - Z_{\dot{q}} & 0 \\ 0 & -mz_g & my_g & I_{xx} - K_{\dot{p}} & 0 & 0 \\ mz_g & 0 & -mx_g - M_{\dot{w}} & 0 & I_{yy} - M_{\dot{q}} & 0 \\ -my_g & mx_g - N_{\dot{v}} & 0 & 0 & 0 & I_{zz} - N_{\dot{r}} \end{bmatrix}^{-1}, \tag{3.16}$$

$$\begin{bmatrix} \dot{u} \\ \dot{v} \\ \dot{w} \\ \dot{p} \\ \dot{q} \\ \dot{r} \end{bmatrix} = A \begin{bmatrix} F_x \\ F_y \\ F_z \\ M_x \\ M_y \\ M_z \end{bmatrix}. \tag{3.17}$$

In the simulation developed, the vehicles move along a predetermined path. The leader-follower approach is implemented so that the leader moves in the middle and the followers are on the sides. Appropriate control laws and controllers should be used to keep the vehicles on track at all times. The status of the vehicle should be used as a baseline for comparing results. As the vehicles move along their path, their true positions, velocities and accelerations are obtained from the simulation. The measurements are generated by adding noise to the true accelerations for the IMU model. Noise is added to the true position difference for acoustic measurements. The ground truth of the vehicles can be seen in Figure 3.3.

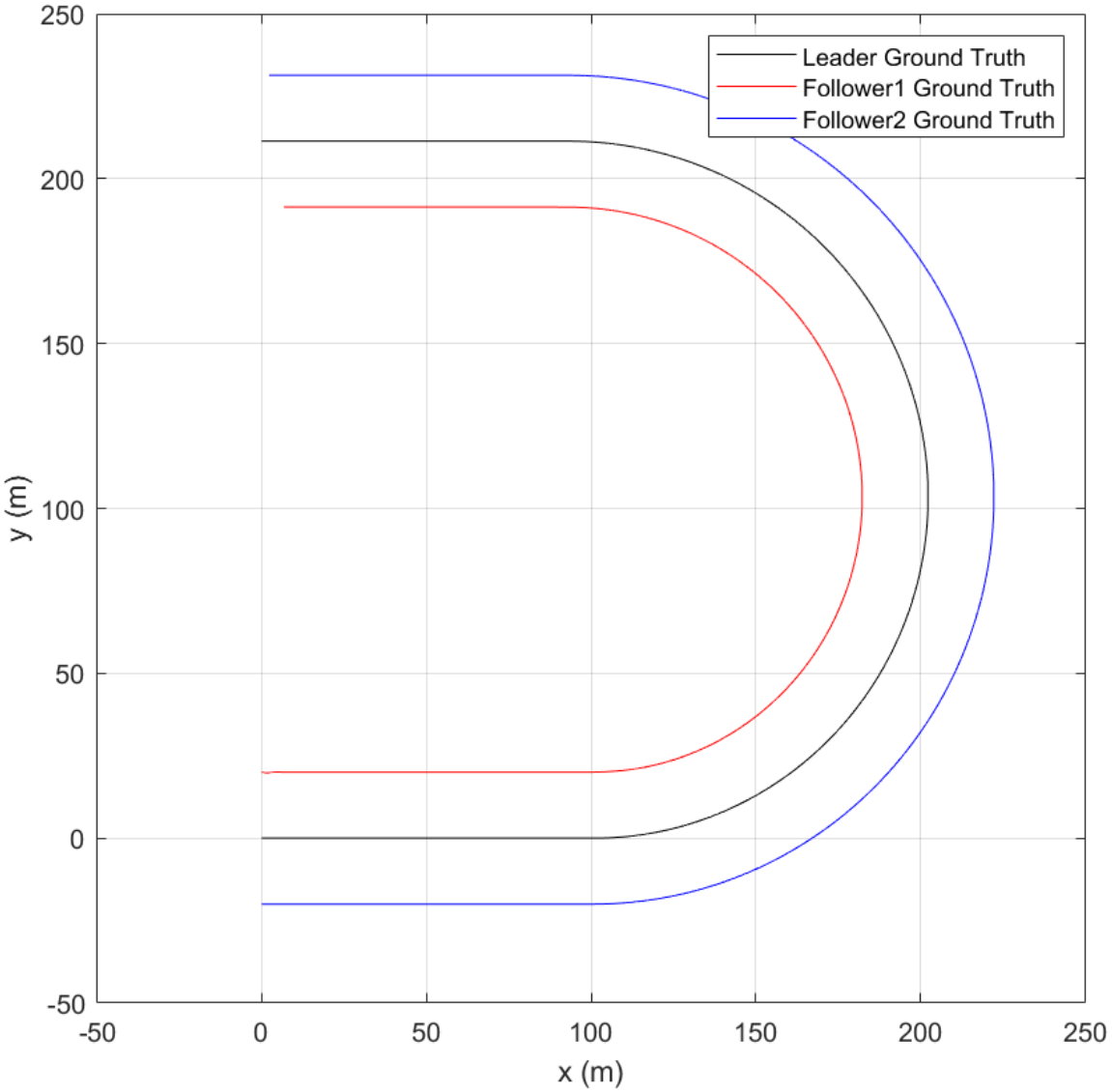

Figure 3.3. Leader and follower trajectories represented by red, black and blue lines. These trajectories are given to the leader and the follower AUVs.

3.4. Experimental Setup

3.4.1. AUVs

The experimental setup consists of 2 underwater vehicles acting as a leader and a follower. The vehicles are rigidly connected to each other so that their relative positions do not change during the course. This application ensures that the relative positions of the vehicles are the same at all times and serves as ground truth. The leader ROV used in the experiment is shown in Figure 3.4. The follower AUV is a sealed tube

rigidly connected to the leader as shown in Figure 3.5. After calibrating the sensors, the AUVs were initialized so that they were separated by one meter on the lateral axis and 0.15 meter on the longitudinal axis. They traveled together at a constant speed along the long side of the basin.

Figure 3.4. Picture of the ROV "Kaplumbot".

3.4.2. Sensors

There are two types of sensors in this research. IMUs that gives acceleration measurements are the first type. Second type is a sonar that measures the distance between two AUVs to obtain relative positions.

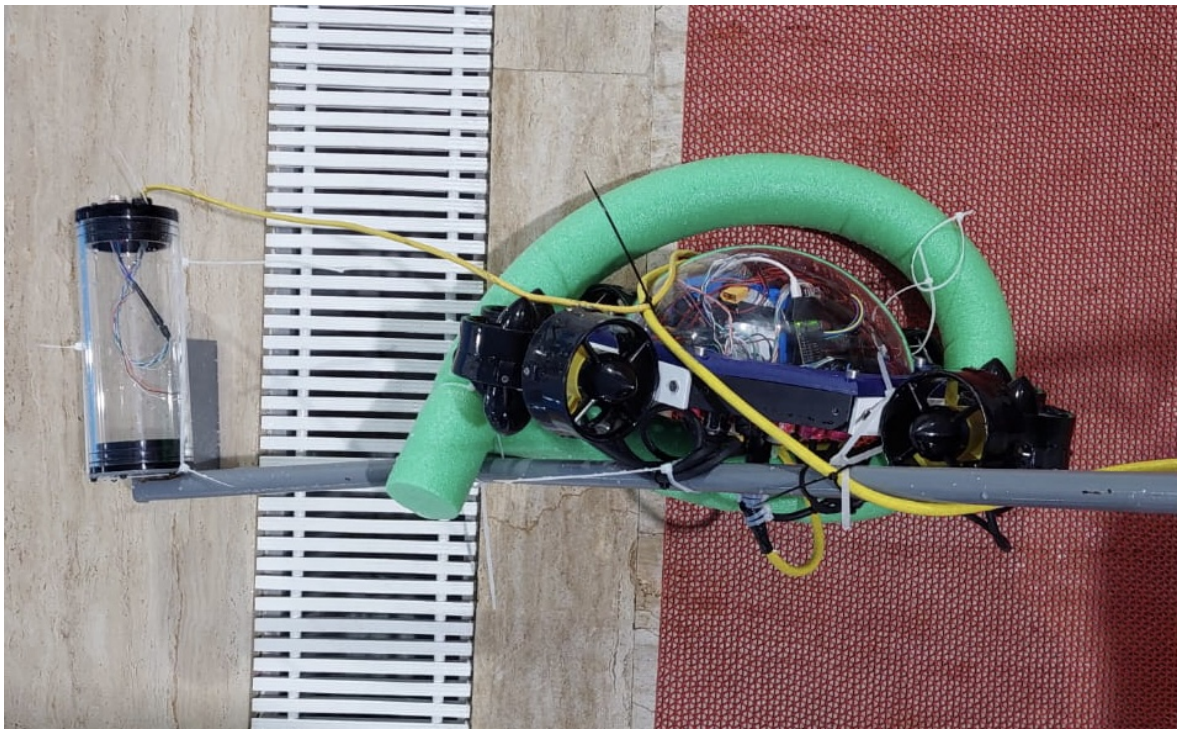

Figure 3.5. Rigid connection of the two AUVs.

Two types of IMU is used in this study. The leader AUV has Pixhawk on-board IMUs and the follower AUV has MPU6050 IMUs mounted. Each vehicle obtains their accelerations with the IMUs that they are equipped with. Each IMU provides vehicle accelerations defined on sensor frame. The sensor frame has three orthogonal axis. If orientations of sensor frames and their respective body fixed frames, a rotation matrix should be constructed. This rotation matrix provides a transformation for acceleration measurements from sensor frame to body fixed frame.

Ping-360 Scanning Imaging Sonar is a commercial product that produces range measurements by the angle. It scans the desired angular range and calculates the distance by reflecting the ToA of the sound waves it generates. Acoustic measurements are provided by a Ping360 sonar sensor to overcome the strong echoes generated by a single transponder in a semi-Olympic-sized swimming pool. A picture of Ping-360 sonar is given in Figure 3.6.

Figure 3.6. Ping-360 sonar by BlueRobotics.

The reason why a sonar is used instead of beam forming is that a commercial transponder generates strong echoes in a pool. These echoes attenuates or fades slowly in a small closed environment. Even though several solutions such as filtering by wave amplitude can be applied to overcome the echoes, using a sonar is much simpler than applying signal processing methods. The main idea here is to obtain acoustic measurements between the AUVs and using a sonar is more suitable in a closed environment.

3.4.3. Acceleration Measurements

The accelerations of the vehicles in 2 dimensions are measured by IMUs. These IMU readings give accelerations in the xyz Cartesian plane. However, these measurements are defined in the body-fixed frame of the vehicle. The accelerations should be multiplied with a rotation matrix to obtain accelerations in the earth-fixed frame.

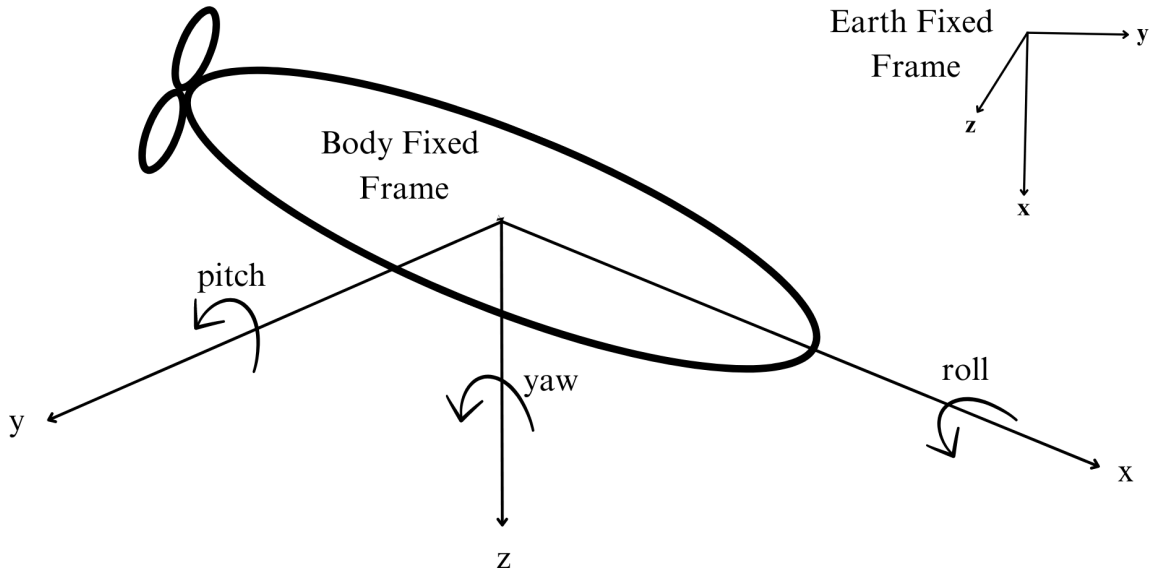

Figure 3.7. Earth-fixed and body-fixed frames [31].

The rotation matrix is constructed from the the orientations of the vehicle. The Euler angles which are roll (ϕ), pitch (θ) and yaw (ψ) must be known for the rotation matrix. Therefore, the assumptions in Section 3.1 should be satisfied. The definitions of the axes and frames are shown in Figure 3.7. The accelerations in the earth-fixed frame are calculated by

$$\begin{bmatrix} a_x \\ a_y \\ a_z \end{bmatrix}_{earth} = R(\phi,\theta,\psi) \begin{bmatrix} a_x \\ a_y \\ a_z \end{bmatrix}_{body} , \tag{3.18}$$

where the rotation matrix $R(\phi,\theta,\psi)$ is constructed by

$$R(\phi,\theta,\psi) = \begin{bmatrix} c(\theta)c(\psi) & s(\phi)s(\theta)c(\psi) - c(\phi)s(\psi) & s(\psi)s(\phi) + c(\psi)s(\theta)c(\phi) \\ c(\theta)s(\psi) & s(\psi)s(\theta)s(\phi) + c(\psi)c(\phi) & c(\phi)s(\theta)s(\psi) - s(\phi)c(\psi) \\ -s(\theta) & s(\phi)c(\theta) & c(\theta)c(\phi) \end{bmatrix} . \tag{3.19}$$

In Equation (3.19) s is the sine function and c is the cosine function. When the rotation matrix $R(\phi,\theta,\psi)$ is multiplied with the accelerations that are measured in the body-fixed frame, the accelerations in the earth-fixed frame are obtained.

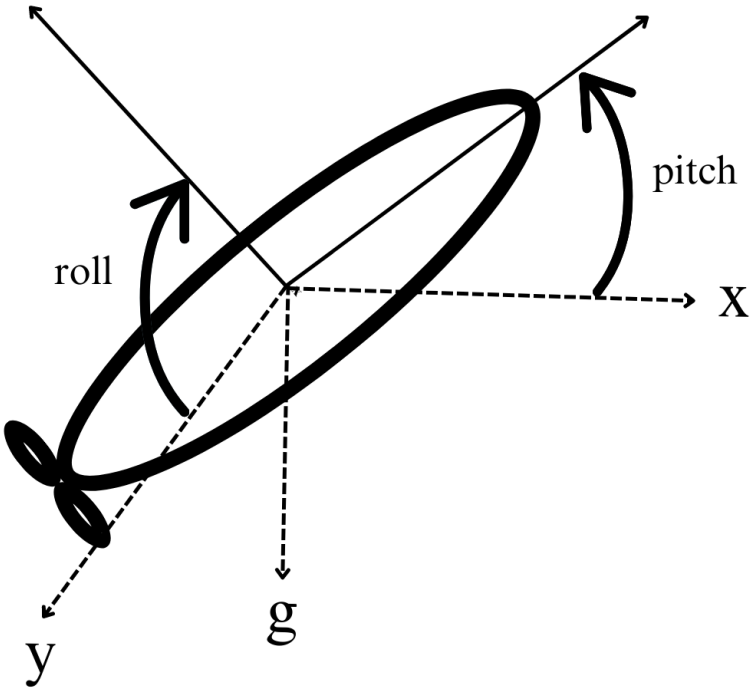

Figure 3.8. Orientation from gravity [32].

Euler angles are obtained from the accelerometers during the experiment. Roll angle and pitch angles can be calculated from the orientation of the vehicle and the gravity. The only acceleration the vehicles have is the gravity since they are moving on a steady course. Since the gravity has a constant value and a direction, its components in the body-fixed frame yield roll and pitch angles as shown in Figure 3.8.

Acceleration components in body-fixed frame and the gravitational acceleration are sufficient to calculate orientation. The roll and pitch angles can be found from trigonometric calculations as:

$$\phi = tan^{-1}\left(a_y^b / a_z^b\right), \tag{3.20}$$

$$\theta = sin^{-1}\left(a_x^b / g\right). \tag{3.21}$$

In the Equations (3.20) and (3.21), tan^{-1} and sin^{-1} are the inverse functions of the tangent and the sine functions respectively.

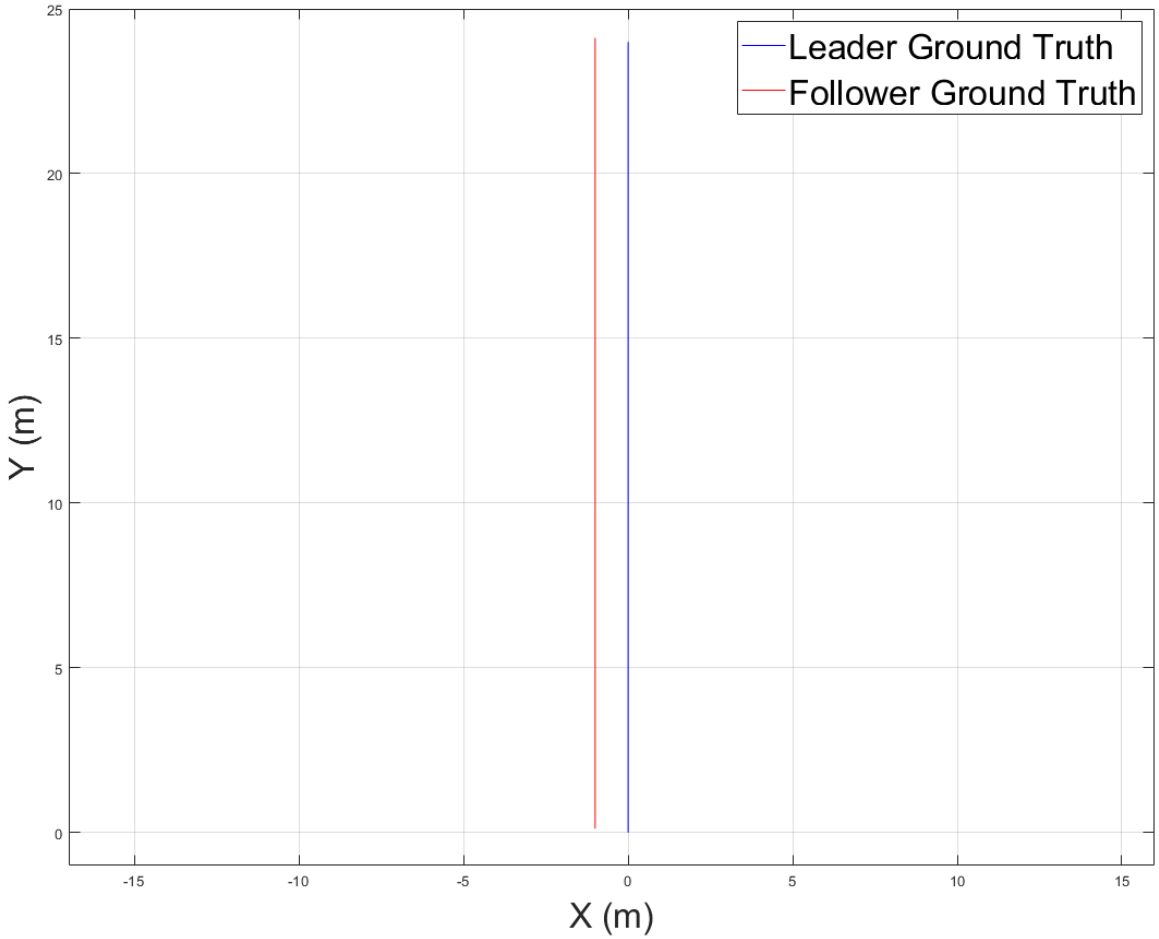

Figure 3.9. Trajectories of the AUVs represented with blue and red lines. These trajectories are given to the leader and the follower AUVs.

The yaw angle cannot be calculated using this approach. Any rotation about the z-axis does not provide any components of gravity on the other axes. The yaw angle must be obtained by other methods. The vehicles move in a straight line during the experiment. The yaw angle is known and constant throughout the course. The ground truth with constant yaw angle of the vehicles is shown in Figure 3.9.

3.4.4. Acoustic Measurements

Acoustic measurements are provided by the Ping-360 Scanning Imaging Sonar. Normally, a single transponder and 3 transducers are sufficient, as suggested in Section 3.1. However, the most of the commercial transponders generates strong waves that echo in the pool for a long time before they fade.

The sonar has a capability of performing range measurements at 0-360 degrees angular range in 2 dimensions. It generates sound waves in series and calculates the ToA of the waves reflected from an object. The waves are generated by a transponder inside and received by a transducer at the same location. The transponder and the transducer is rotated mechanically by a actuator and scanning repeats. By this method, a full 360 degrees scan is obtained. During the experiment, 13 degrees of is sufficient to measure the relative distance between the AUVs. Limiting the scanning angle range increases measurement frequency since a full scan requires a lot of time because of mechanical rotation.

The measurements are obtained in polar coordinates, since they are given in the form of a distance and an angle, and it should be transformed into Cartesian coordinates. A distance measurement is recorded for each angular increment by

$$x_i = r_i cos(\beta_i), \tag{3.22}$$

$$y_i = r_i sin(\beta_i). \tag{3.23}$$

The transformation from the polar coordinates to the xy plane is given by Equation (3.22) and Equation (3.23). The vehicle's relative position from its center can be found when the i^{th} angle is the bisector, as in

$$\beta_i = \frac{\beta_{max} + \beta_{min}}{2}. \tag{3.24}$$

The center that found by Equation (3.24) is illustrated in Figure 3.10. The bisector center is determined to the vehicles position. The relative distance and position measurements in Equation (3.9) corresponds to the bisector center.

3.4.5. Electronics and Software

The leader AUV has a microcontroller, Nvidia Jetson Nano, and a flight control unit Pixhawk. The Nvidia Jetson Nano has its own Linux-based operating system. It communicates with Pixhawk and Ping360 Sonar.

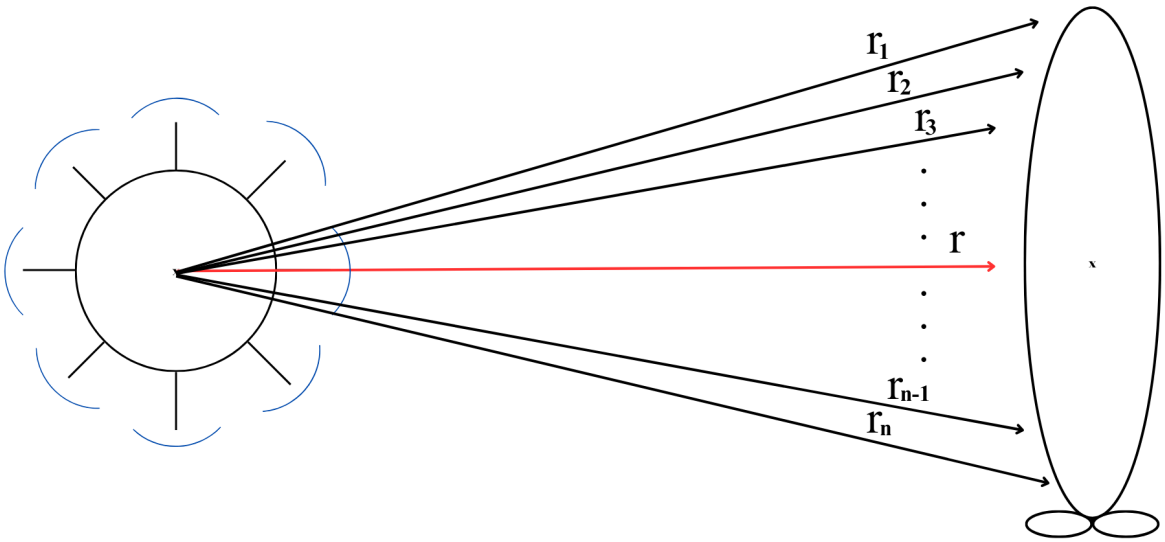

Figure 3.10. Central position measurement by bisector angle which is shown by the red arrow.

The Pixhawk flight controller has an on-board IMU unit that measures accelerations with the accelerometers and orientations with the magnetometers. It is also capable of generating motor inputs with its PID controller units. Both Ping360 Sonar and Pixhawk are connected to the Nvidia Jetson Nano via USB ports.

The follower AUV is connected to the microcontroller. The MPU IMU communicates with the microcontroller via its SDA/SCL ports. I^2C communication is established between the IMU and the microcontroller. Information exchange can be done with acoustic waves between a transponder and a transducer couple. However, in the proof-of-concept experiment, a cable connection is established between two AUVs.

Acoustic modems that are commercially available can be another method for acoustic communication. Underwater communication is a rapidly growing topic. The most important features that are being developed are data transmission rate and maximum available distance. Some of the commercial products of acoustic modems are tabulated in Table 3.1 [33].

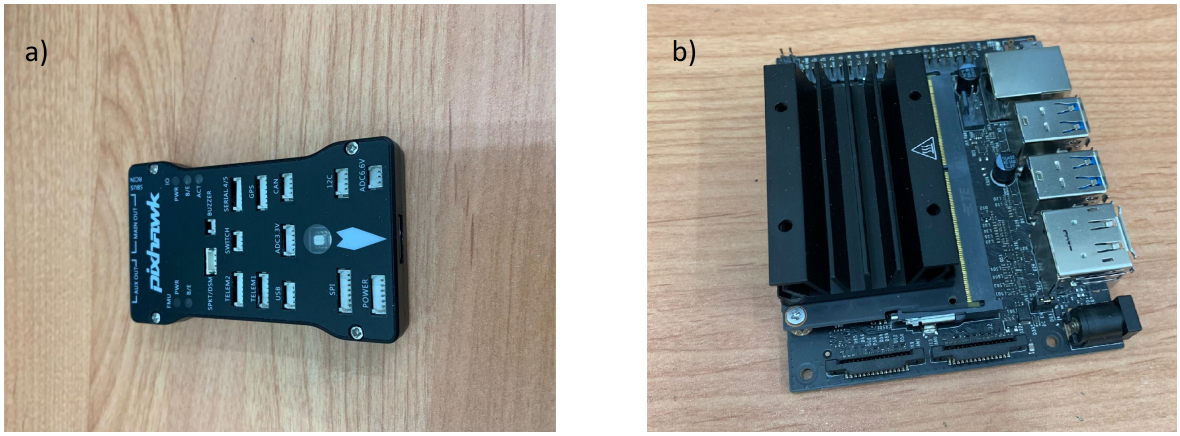

Figure 3.11. (a) A picture of Pixhawk flight controller, (b) A picture of Nvidia Jetson Nano micro-controller unit.

Table 3.1. Commercially available acoustic modems and their features [33].

Product Name	**Carrier Frequency**	**Bandwith**	**Data Rate**	**Max Distance**
Aquatec AQUAModem	9.75 kHz	4.5 kHz	2000 bps	5000 m
DSPComm AquaComm Orca	14 kHz	100 kHz	0.007 bps	3000 m
Desert Star Systems SAM-1	37.5 kHz	9 kHz	154 bps	1000 m
EvoLogics S2CR 18/34wise	18-34 kHz	16 kHz	139000 bps	3500 m
LinkQuest UWM10000	10 kHz	5 kHz	5000 bps	10000 m
Teledyne Benthos Atm9xx	18.5 kHz	5 kHz	15360 bps	6000 m

The data acquisition software is written in Python. It runs at 100 ms to collect measurements from IMUs. The Ping360 sonar runs much slower, taking a new measurement about once every 500 ms. The last measurement is considered valid until a

new measurement is obtained. All data from the IMU, Pixhawk, and Ping-360 Sonar is recorded and analyzed off-board.

3.5. Experimental Procedure

During the experiment, three separate trials are completed. Same procedure is followed for each trial with the same initial conditions. Similar environmental conditions are held during the trials to achieve consistent results. The same setup is used for mechanical and electronic components.

The experiment takes place in a semi-olympic size pool. Two AUVs are rigidly connected with a metal bar as shown in Figure 3.5. This rigid bar keeps the relative distance between two AUVs constant. These AUVs are initialized at the corner of the pool. They move at a constant speed and heading alongside the long edge of the pool. While they are moving, the acoustic sensor takes distance measurements which are used to find the relative locations as shown in Figure 3.10. Also, IMUs that are mounted on AUVs are getting acceleration measurements. These measurements from both acoustic sensor and IMUs are recorded by the Python code running on Nvidia Jetson Nano.

The recorded data is analyzed to obtain DR location outputs and RN location outputs. Acceleration measurements are integrated twice to derive the follower AUV's DR results. These results are plotted. RN uses both acceleration measurements and acoustic measurements as given by Equation (3.9). The location of the follower AUV according to RN is plotted as well. Both RN and DR locations are compared with the ground truth of the vehicles given in Figure 3.9. The deviation between true path and location calculations are considered as the error of the navigation system.

4. RESULTS

4.1. Simulation Results

Each vehicle's IMU model outputs, which are acceleration measurements, are integrated twice to obtain DR measurement results in the simulation. As shown in Figure 4.1, the vehicles are subject to navigational drift. Due to the integration of the noise terms, the DR navigation is subject to the random walk and drifts over time as expected.

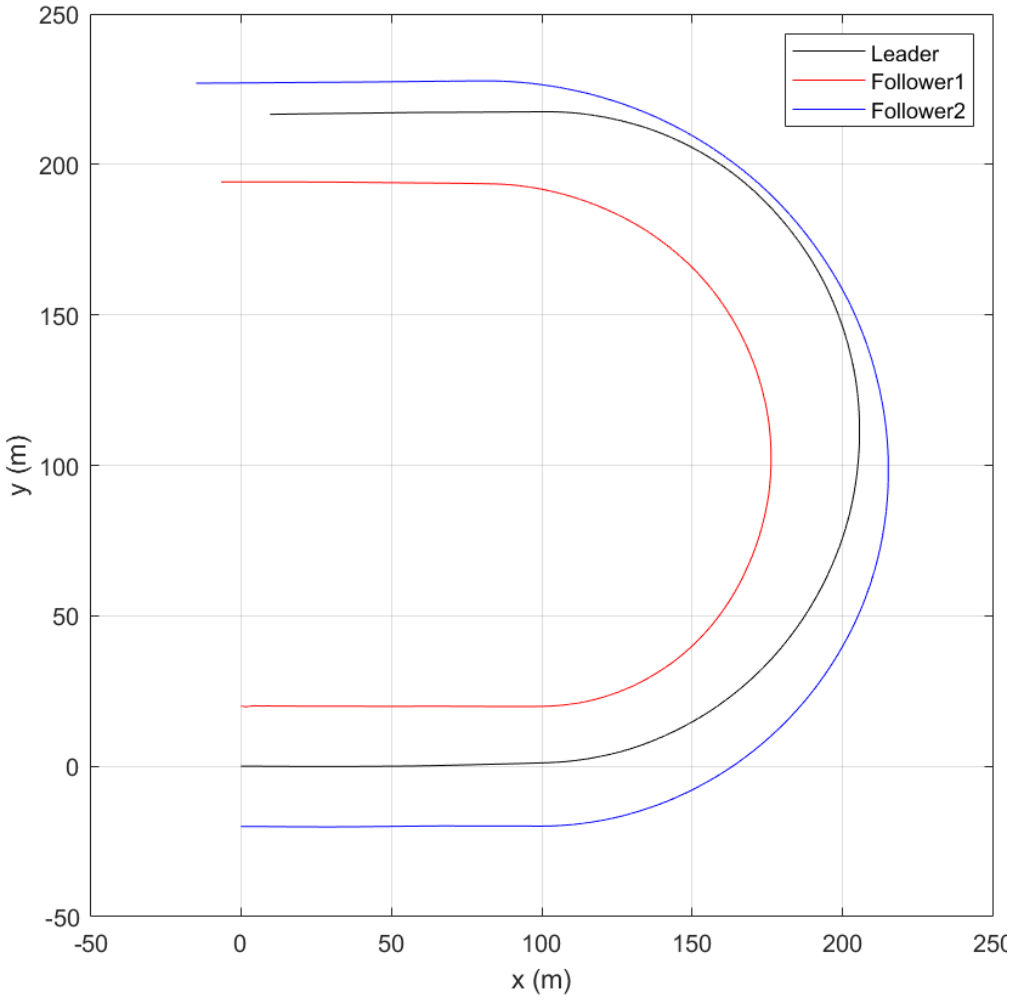

Figure 4.1. Leader and follower position estimation results calculated by dead reckoning navigation.

The initial formation is broken and the vehicles come dangerously close to each other. However, with the help of the acoustic range measurements and state estimation, the formation is maintained and coordinated maneuvers are realized as shown in Figure 4.2. Relative position error is minimized and relative navigation is achieved. The followers follow the formation rules even if the leader deviates from the original predefined path. The simulation results show that a relative position measurement is necessary to maintain the formation of the vehicles. Dead reckoning, even with high quality accelerometers, is not suitable for long voyages.

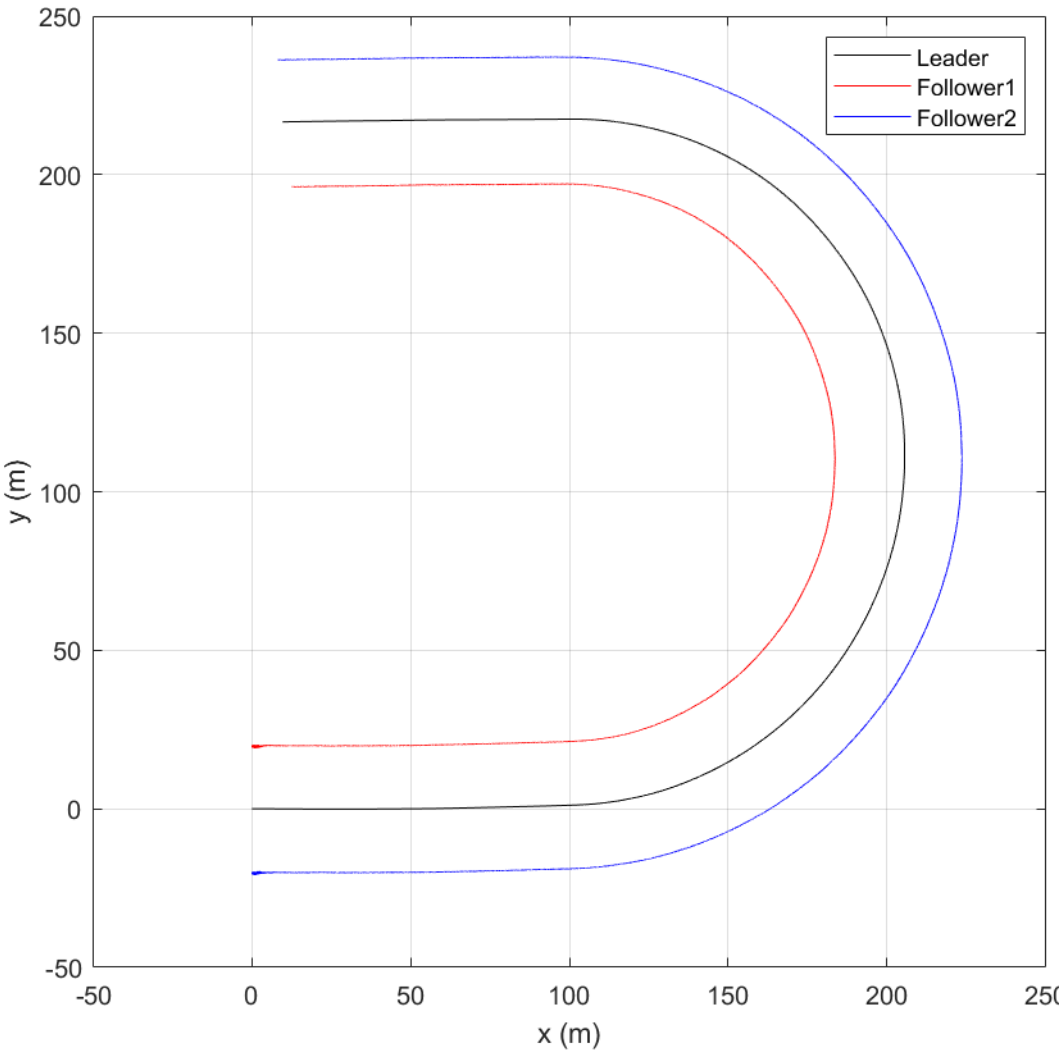

Figure 4.2. Leader and follower position estimation results calculated by relative navigation.

As seen in Figure 4.3, the followers' errors reaches up to 18 meters while they initially start from 20 meters separation. The followers do not catch up with the deviation of the leader from its original path because there is are correction terms. On the other hand, the relative navigation algorithm and the acoustic measurements provide a relative position error correction term. When the leader maneuvers, they keep up with it. The coordinated movements are realized with only a few centimeters of error.

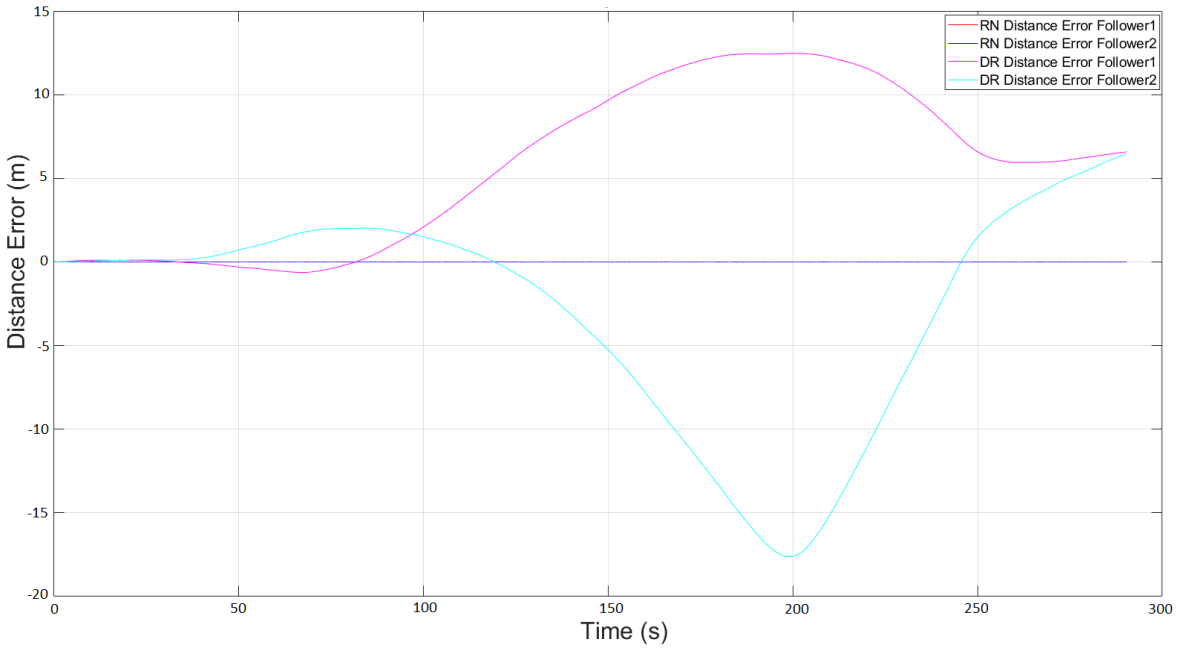

Figure 4.3. Distance error of both followers calculated by DR and Relative Navigation methods

4.2. Experimental Results

Three distinct trials are done with the setup described in Section 3.4. The collected data is plotted. Positions of the follower AUV is given by both DR and RN methods. DR and RN method position outputs are compared with the ground truth of the follower AUV.

4.2.1. First Trial

The first trial results are shown in Figure 4.4 and the Figure 4.5. The ground truths are shown with black lines. The leader's own navigation is shown with a blue line. The follower's dead reckoning results are shown with a dashed red line. As can be seen in Figure 4.4, the navigational drift of the follower causes the formation between the two vehicles to be broken. The leader, which has a better IMU, drifts a little from its original path, while the follower, which has a less expensive IMU, drifts much more.

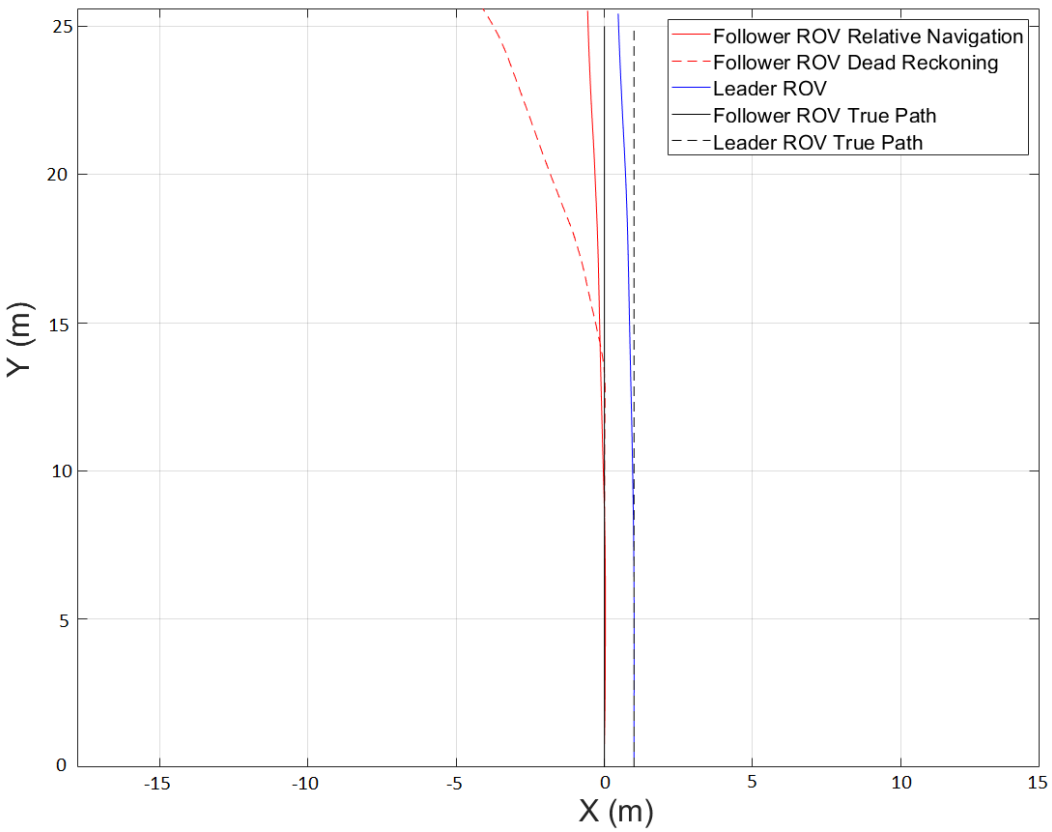

Figure 4.4. Dead reckoning and relative navigation results from first trial.

The acoustic measurement updates eliminate the drift and keep the formation intact. During even a short voyage, the relative distance error approaches four meters in the dead reckoning approach, as shown by the blue line in Figure 4.5. However, the proposed method provides less than 10 cm range error as shown by the red line in Figure 4.5.

The acoustic measurement and the velocity updates are also provided for each experiment. According to the 2D model provided in Section 3.1, two relative distances and two relative velocities are measured.

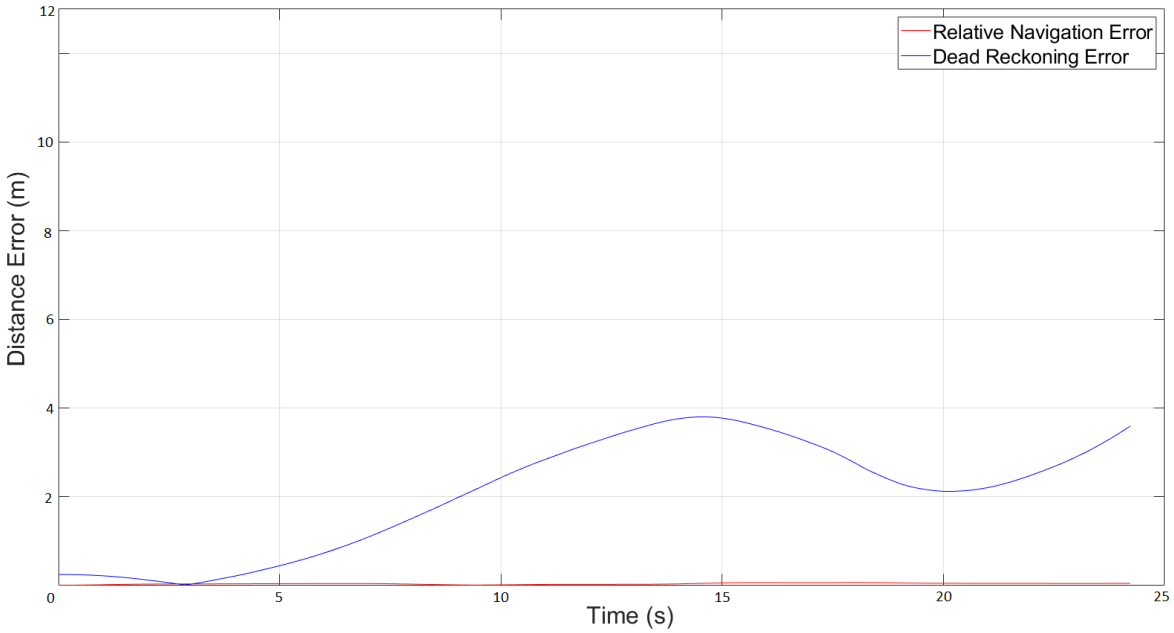

Figure 4.5. Dead reckoning and relative navigation error from first trial.

According to Equation (3.9), the relative positions x_{rel}, y_{rel} and the relative velocities $\dot{x}_{rel}$, $\dot{y}_{rel}$ come from the acoustic measurements. The acoustic measurements are obtained as explained in Section 3.4.4. The acoustic relative distances and the velocities are consistent with the ground truths. One meter on the x-axis and 0.125 meters on y-axis is seen in Figure 4.6. The relative velocities are zero as shown in Figure 4.7, which is true considering that the AUVs are rigidly connected.

When the Figure 3.9 and 4.4 are compared, the Relative Navigation system gives consistent results with the true path. An error in the centimeter range is achieved. This level of error is acceptable when compared to the dimensions of the AUVs.

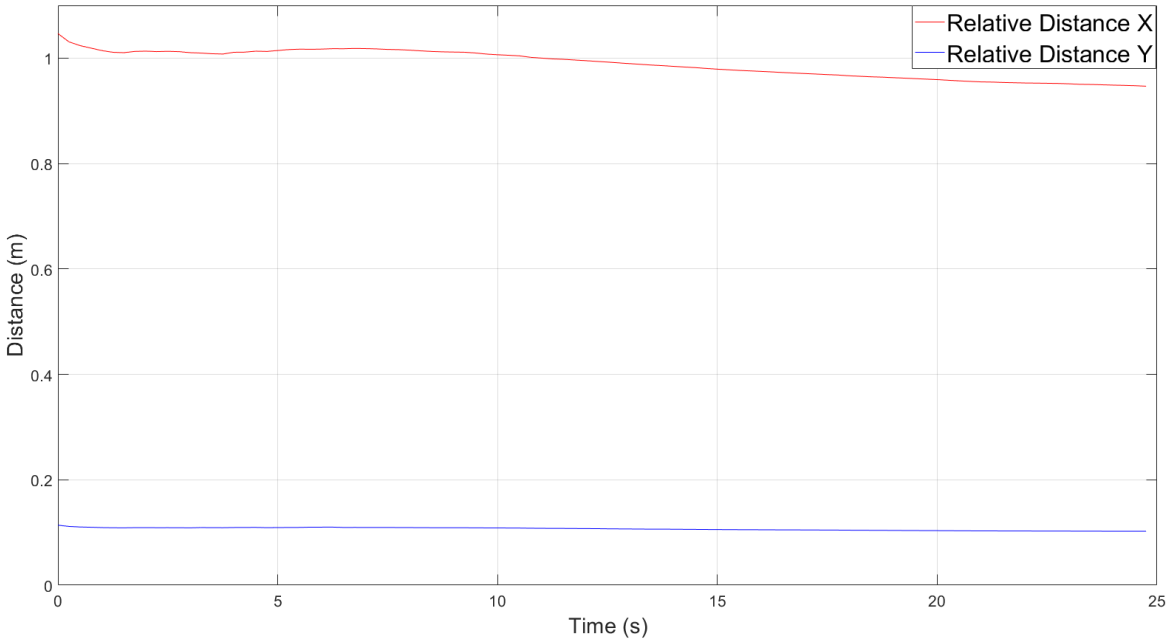

Figure 4.6. Acoustic distance measurements from first trial.

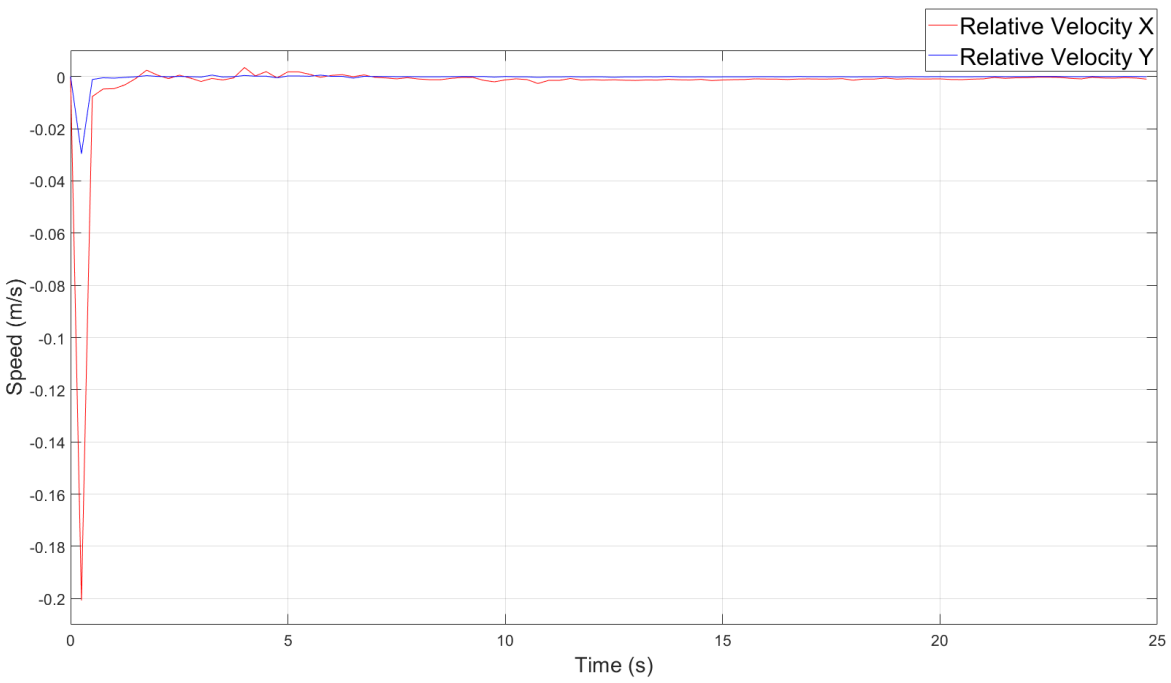

Figure 4.7. Acoustic velocity measurements from first trial.

4.2.2. Second Trial

The same procedure is repeated in the second trial and the results are shown in Figure 4.8 and Figure 4.9. The leader with better IMU shows much better positioning than the follower AUV. On the other hand, the follower drifts from its path according to DR navigation. The Figure 4.9 shows that the relative distance error exceeds three meters. Even for a short voyage with no maneuvers, the formation does not exist.

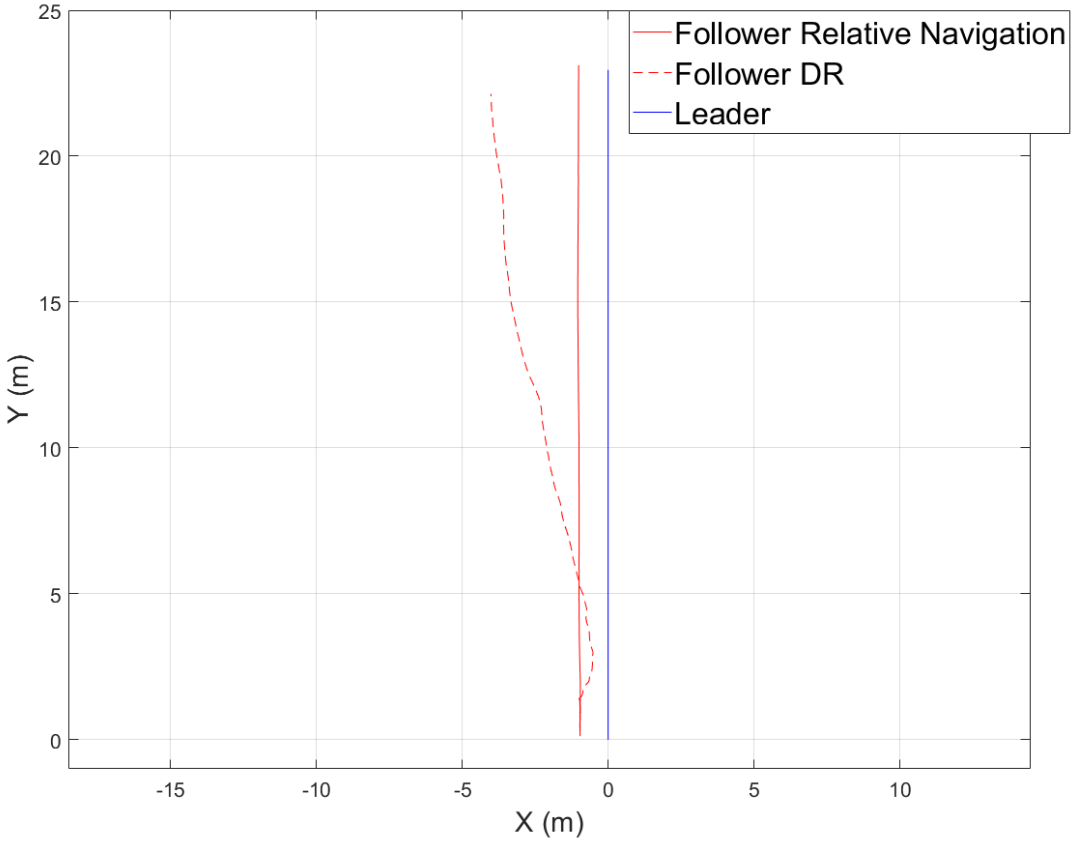

Figure 4.8. Dead reckoning and relative navigation results from second trial.

When the Relative Navigation algorithm is used, the results are much better than the DR navigation results for the follower AUV. The formation is preserved as shown in Figure 4.8.

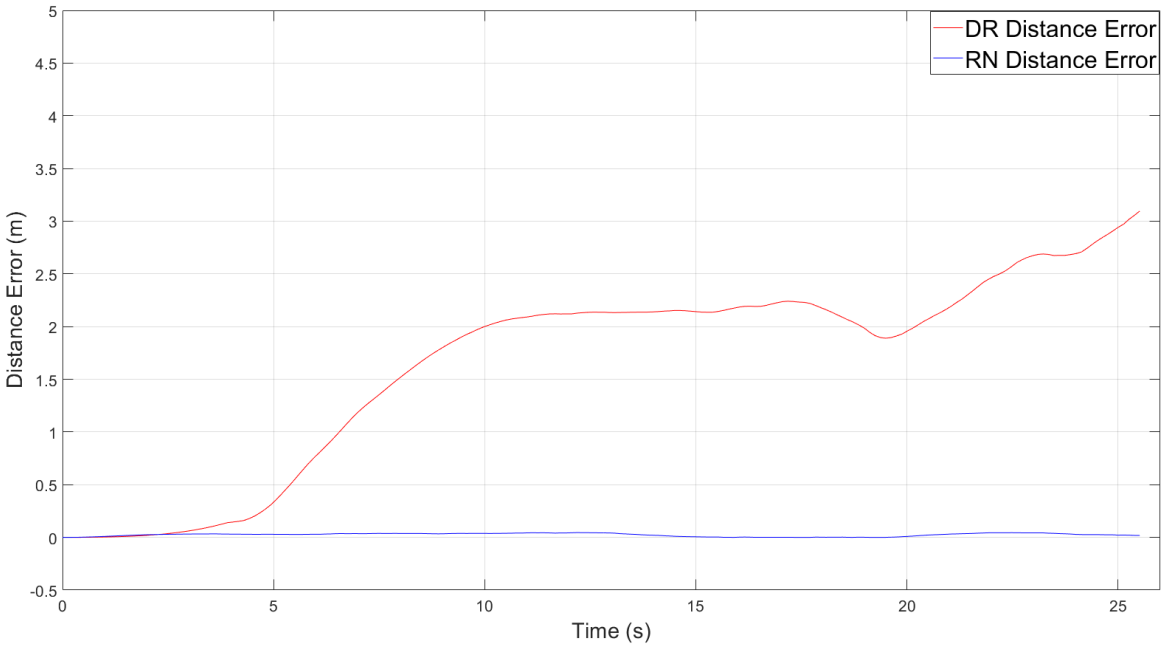

Figure 4.9. Dead reckoning and relative navigation error from second trial.

The ground truth, shown by Figure 3.9 is compared with the localization results that can be seen in Figure 4.8. Similar conclusions can be deducted from the first trial. The relative position error for the RN system does not exceed a few centimeters. However, DR localization results have meter level error.

The relative distance error fluctuates by only a few centimeters, as shown with the blue line in Figure 4.9. The relative distance measurements are correctly updating the navigation algorithm as shown in Figure 4.10 and the relative velocities are zero as expected from the Figure 4.11.

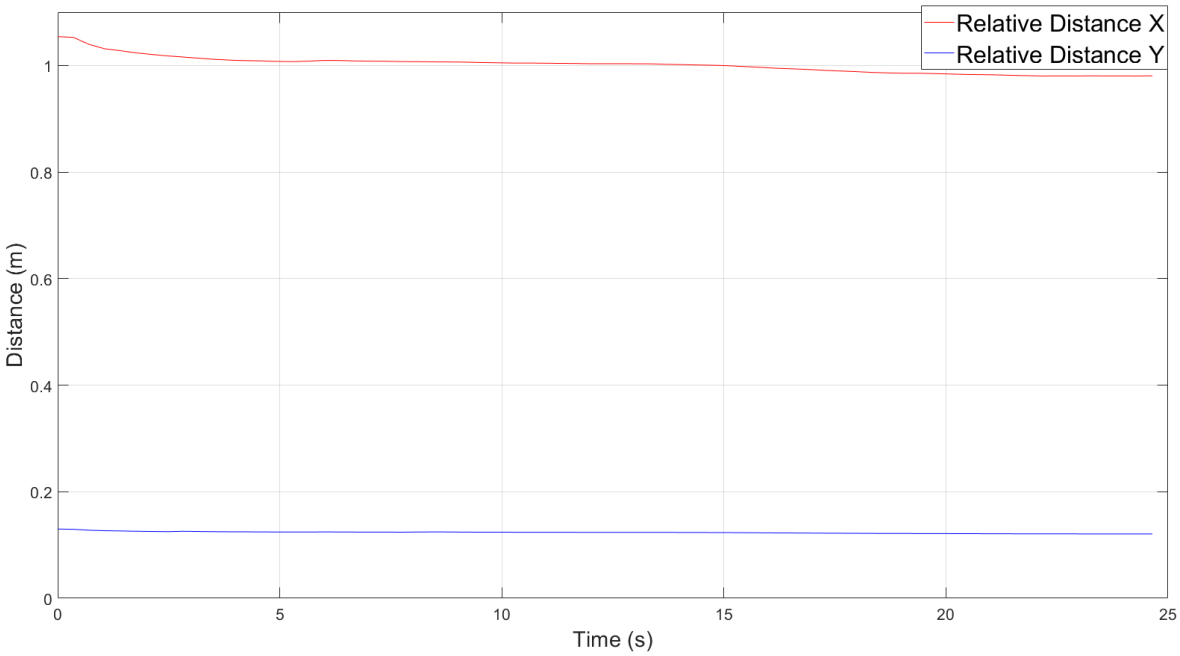

Figure 4.10. Acoustic distance measurements from second trial.

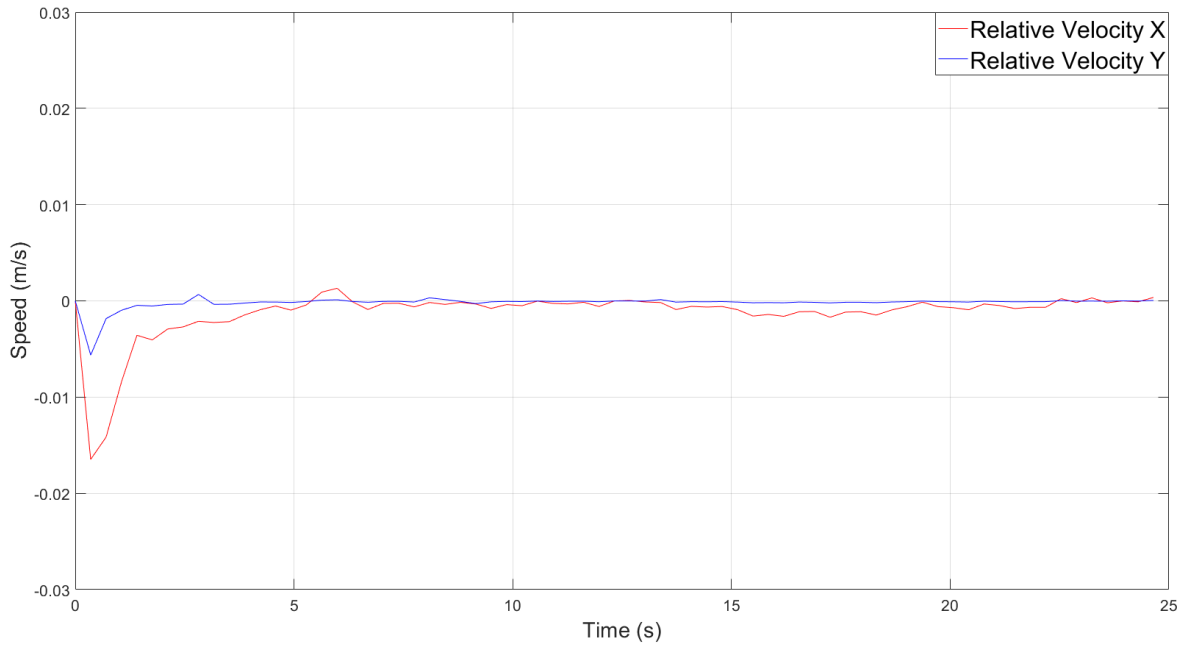

Figure 4.11. Acoustic velocity measurements from second trial.

4.2.3. Third Trial

The last trial shows the similar results with the first and the second one. The same process is applied and the localization results of both DR and RN are plotted as seen in Figure 4.12 and Figure 4.13. The follower and leader AUVs approach each other so close at the beginning that they are about to collide according to the DR navigation results as shown by the dashed red line in Figure 4.12. At the second half the voyage, they drift apart. The formation is broken and their error becomes close to five meters as shown in Figure 4.13.

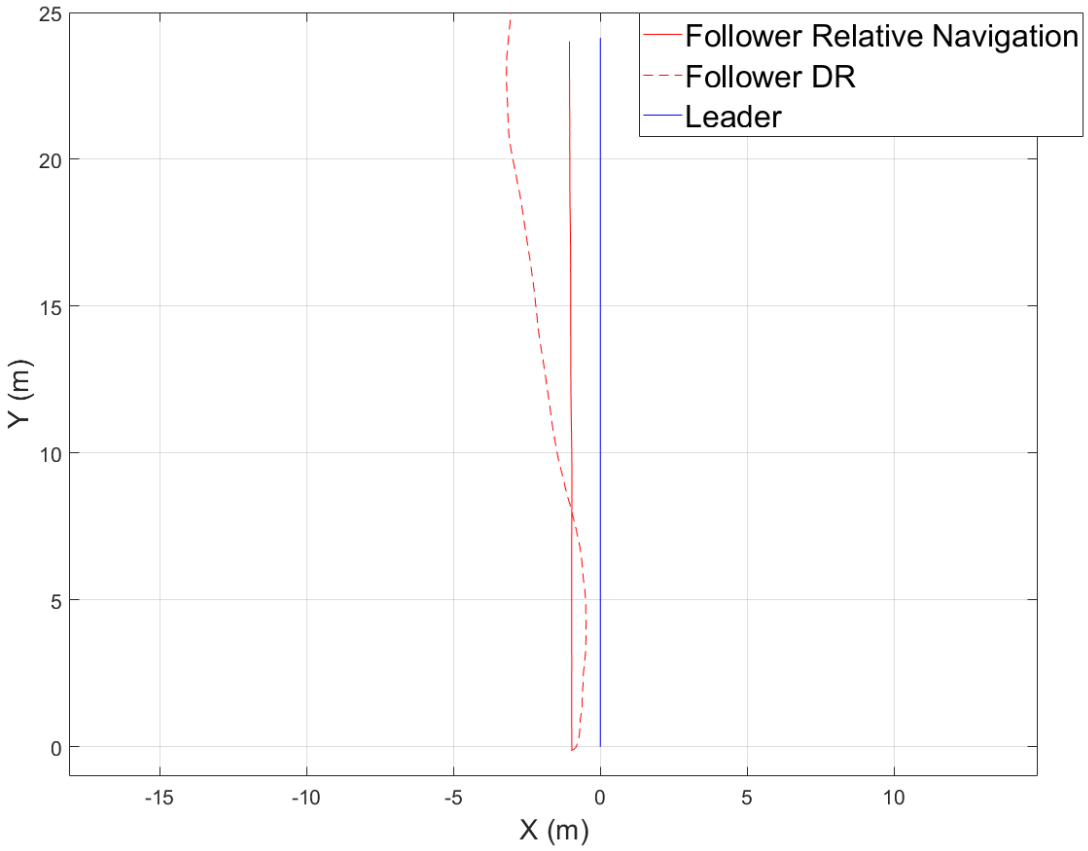

Figure 4.12. Dead reckoning and relative navigation results from third trial.

According to the Relative Navigation algorithm, the positioning of the follower AUV is much better. Initial formation is intact as seen in Figure 4.12. The relative position error is negligible compared to the AUV sizes. It does not exceed six centimeters.

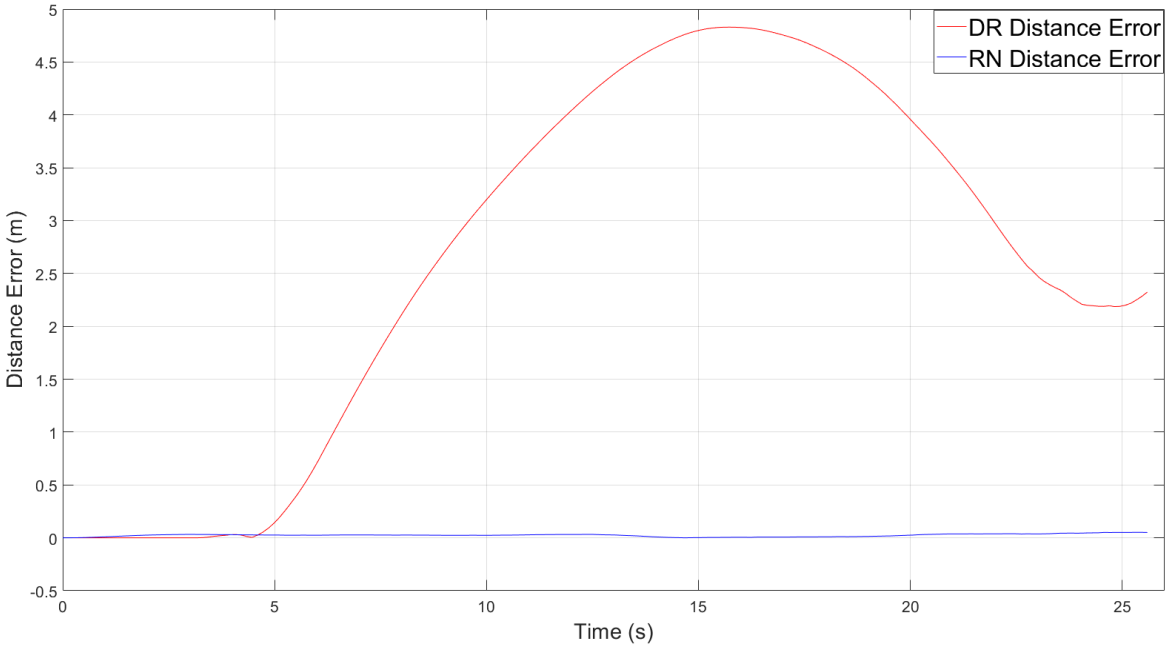

Figure 4.13. Dead reckoning and relative navigation error from third trial.

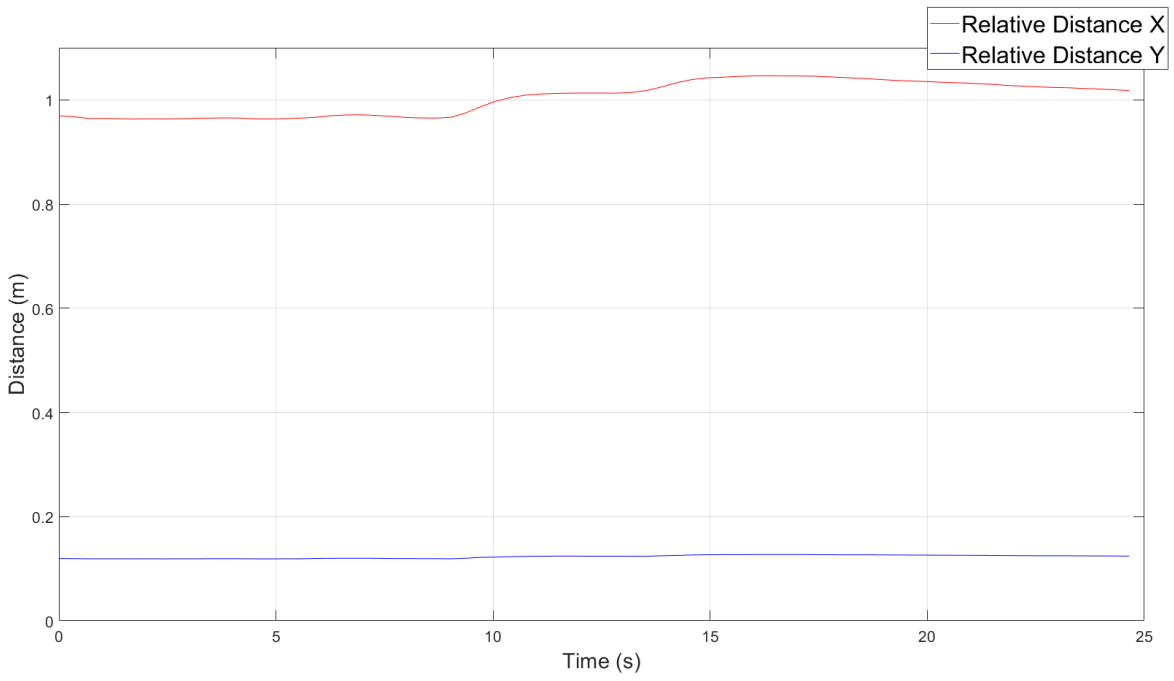

Figure 4.14. Acoustic distance measurements from third trial.

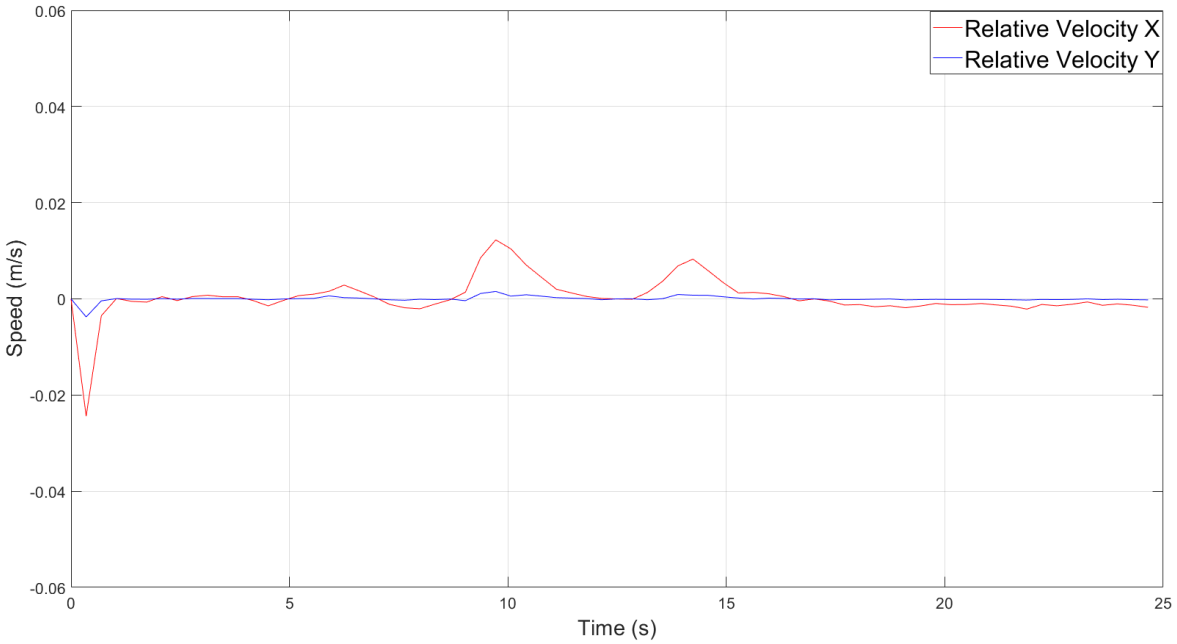

Figure 4.15. Acoustic velocity measurements from third trial.

The acoustic distance measurements in Figure 4.14 are compatible with the true positions of the AUVs. The acoustic velocities oscillate around zero as shown in Figure 4.15. Since the AUVs are rigidly connected to each other, there should be no relative motion. The measurement updates are as expected.

4.3. Discussion

Three of the trials show that the proposed system yields much better results compared to DR navigation. Followers position themselves according to the leader while keeping their formation preserved. An acoustic measurement is found to be useful and necessary even for a short voyage. Error analysis is summarized in the table below.

Table 4.1. Mean distance error and standard deviation from three trials according to DR and RN results.

	Mean Error (m)	**Standard Deviation (m)**
1^{st} **Trial DR**	2.1200	1.4255
1^{st} **Trial RN**	0.0235	0.0092
1^{st} **Trial without Kalman**	0.0860	0.0139
2^{nd} **Trial DR**	1.6405	0.9282
2^{nd} **Trial RN**	0.0104	0.0080
2^{nd} **Trial without Kalman**	0.0172	0.0138
3^{rd} **Trial DR**	2.6475	1.7422
3^{rd} **Trial RN**	0.0101	0.0072
3^{rd} **Trial without Kalman**	0.0133	0.0129

As seen from Table 4.1, mean error of RN navigation is negligible compared to AUV dimensions. Each trials show that acoustic measurements improve the localization of the follower AUVs. Additional improvement is expected from the Kalman filter algorithm that is used to fuse acoustic measurements with IMU readings. To understand its contribution, Kalman filter can be disabled. The follower AUVs can navigate with their IMU sensor as in DR navigation until an acoustic measurement is obtained. Once acoustic position knowledge is obtained, the position of the follower can be updated. Then the same procedure repeats itself. This method does not rely on any fusing algorithm or filtering.

Kalman filter is used to reduce noise effects on a system. If the Kalman filter is disabled, position estimation is calculated by IMUs between two acoustic measurements. When RN results are compared with results without Kalman in Table 4.1, it seems that Kalman filter slightly reduces distance error level.

The results clearly shows that the proposed system in this study yields far better results than relying on only IMU measurements and estimation from DR only. However, one should notice that all experiments are conducted in a very controlled environment.

AUVs are rigidly connected to each other and cable connection is established. Beam forming with a sonar is used in the pool environment instead of trilateration because of the limitations of the swimming pool.

The experimental data is obtained with very controlled conditions. The vehicles are not maneuvering but going on a straight line. The vehicles are rigidly connected to each other. Information exchange between vehicles is very fast due to cable connection. Since the dynamics of the vehicles do not change rapidly and the disturbance on the system are very low, the results are obtained smoothly.

Many challenges may rise if the experiment is conducted in open seas or oceans. The rigid connection between AUVs make sure that vehicles are seperated each other with a known distance. To confirm that, an external position measurement system can be used. LBL is the first alternative to have a position estimation of the AUVs. This system can be useful to observe if AUVs sustain their formation.

Secondly, the cable connection is used to let AUVs communicate with each other. As mentioned in Section 3.4.5, acoustic modems might be useful to take the experiment in open seas. The data that is transmitted from a leader to a follower is small in size. Only IMU readings of the leader AUV with a time stamp, which is 4 float variables, are enough for communication. Even though commercial systems are available for the task, the transmitted data might suffer from package losses, interferences and delays due to background sound, wave attenuation, signal blocking and reflected waves.

The objective of this study is to construct a low-cost navigation system that significantly reduces relative position errors for a multi-vehicle environment. A navigation system with acoustic measurements and data fusion is constructed. Although the experimental trials are conducted in a controlled environment, both simulation and experimental results are strongly promising that the proposed navigation system is a huge improvement for reducing position errors.

5. CONCLUSION

The aim of this research was to propose a navigation system for a multi-vehicle underwater environment using relative positioning instead of global positioning. An architecture for a relative measurement system and an algorithm based on state estimation have been developed for this purpose. Experimental and simulation results shows that the proposed system is a much better alternative to conventional DR navigation. Navigational drifts, misalignment errors and bias errors are minimized using this approach.

Simulation and experimental localization results for the follower AUVs are in agreement. The low-cost IMU causes position drift. The errors are caused by misalignment, bias and noise in the acceleration. When a relative position measurement is obtained, the performance of the navigation system becomes much better.

The results show that the position error of the follower AUVs is much better than relying on the commonly used dead reckoning method alone. Even if the lead vehicle deviates from its original path or maneuvers, the proposed solution adjusts the followers accordingly by maintaining their formation control laws. It also provides an acoustic distance measurement from the leader to the followers. A simple transponder and transducer pair is sufficient to achieve this. To eliminate the effects of noise on the system, an extended Kalman gain is used to fuse the kinematic model, IMU readings, and acoustic measurements.

REFERENCES

1. Jalal, F. and F. Nasir, "Underwater Navigation, Localization and Path Planning for Autonomous Vehicles: A Review", *2021 International Bhurban Conference on Applied Sciences and Technologies*, Islamabad, Pakistan, 2021.

2. Melo, J. and A. Matos, "Survey on Advances on Terrain Based Navigation for Autonomous Underwater Vehicles", *Ocean Engineering*, Vol. 139, pp. 250–264, 2017.

3. Marblestone, A., B. Zamft, Y. Maguire, M. Shapiro, T. Cybulski, J. Glaser, D. Amodei, P. Stranges, R. Kalhor, D. Dalrymple, D. Seo, E. Alon, M. Maharbiz, J. Carmena, J. Rabaey, E. Boyden, G. Church and K. Kording, "Physical Principles for Scalable Neural Recording", *Frontiers in Computational Neuroscience*, Vol. 7, p. 137, 2013.

4. Kepper, J., B. Claus and J. C. Kinsey, "A Navigation Solution Using a MEMS IMU, Model-Based Dead-Reckoning, and One-Way-Travel-Time Acoustic Range Measurements for Autonomous Underwater Vehicles", *IEEE Journal of Oceanic Engineering*, Vol. 44, No. 3, pp. 664–682, 2019.

5. Sørensen, F. F., M. von Benzon, S. Pedersen, J. Liniger, K. Schmidt and S. Klemmensen, "Experimental Filter Comparison of an Acoustic Positioning System for Unmanned Underwater Navigation", *IFAC-PapersOnLine*, Vol. 55, No. 36, pp. 25–30, 2022.

6. Ribas, D., P. Ridao, A. Mallios and N. Palomeras, "Delayed State Information Filter for USBL-aided AUV Navigation", *2012 IEEE International Conference on Robotics and Automation*, Saint Paul, MN, USA, 2012.

7. Lee, P.-M., B.-H. Jun, K. Kim, J. Lee, T. Aoki and T. Hyakudome, "Simulation of an Inertial Acoustic Navigation System with Range Aiding for an Autonomous

Underwater Vehicle", *IEEE Journal of Oceanic Engineering*, Vol. 32, No. 2, p. 327–345, 2007.

8. Prikhodko, I. P., B. Bearss, C. Merritt, J. Bergeron and C. Blackmer, "Towards Self-Navigating Cars Using MEMS IMU: Challenges and Opportunities", *IEEE International Symposium on Inertial Sensors and Systems*, Lake Como, Italy, 2018.

9. Wang, M. and Y. Meng, "Research on Angle Random Walk Suppression and Error Estimation and Compensation Method Based on Online Weight Distribution of Multi-RINSs", *IEEE Sensors Journal*, Vol. 22, No. 14, pp. 14470–14480, 2022.

10. Mattern, J., L. Bezanson, V. Nguyen, J. Seawall, R. Conescu and D. Moore, "Underwater Navigation using 3D vision, Edge Processing, and Autonomy", *Oceans 2021: San Diego*, Porto, San Diego, CA, USA, 2021.

11. Beauregard, S. and H. Haas, "Pedestrian Dead Reckoning: A Basis for Personal Positioning", *Proceedings of the 3rd Workshop on Positioning, Navigation and Communication*, Hannover, Germany, 2006.

12. Dell'Erba, R., "The Localization Problem for an Underwater Swarm", 2012, `https://hal.archives-ouvertes.fr/hal-01977313`, accessed on March 19, 2023.

13. Li, L., Y. Li, Y. Zhang, G. Xu, J. Zeng and X. Feng, "Formation Control of Multiple Autonomous Underwater Vehicles Under Communication Delay, Packet Discreteness and Dropout", *Journal of Marine Science and Engineering*, Vol. 10, No. 7, 2022.

14. Li, Y.-P. and S.-X. Yan, "Formation Control of Multiple Autonomous Underwater Vehicles Based on State Feedback", *Proceeding of the 11th World Congress on Intelligent Control and Automation*, pp. 5523–5527, Shenyang, China, 2014.

15. Lawrence, A., *Modern Inertial Technology*, Springer, New York, 1998.

16. Farrell, J. A., *Aided Navigation: GPS with High Rate Sensor*, McGraw-Hill, New York, 2008.

17. Ali, J. and U. B. Mirza, "Performance Comparison Among Nonlinear Filters for a Low Cost SINS/GPS Integrated Solution", *Nonlinear Dynamics*, Vol. 61, 2010.

18. Kinsey, J. C., R. M. Eustice and L. L. Whitcomb, "A Survey of Underwater Vehicle Navigation: Recent Advances and New Challenges", *IFAC Conference of Manoeuvering and Control of Marine Craft*, Vol. 88, pp. 1–12, Lisbon, 2006.

19. Morgado, M., P. Oliveira, C. Silvestre and J. F. Vasconcelos, "Embedded Vehicle Dynamics Aiding for USBL/INS Underwater Navigation System", *IEEE Transactions on Control Systems Technology*, Vol. 22, No. 1, pp. 322–330, 2014.

20. Lee, P.-M., B.-H. Jun and Y.-K. Lim, "Review on Underwater Navigation System Based on Range Measurements from One Reference", *Oceans 2008 - MTS/IEEE Kobe Techno-Ocean*, pp. 1–5, Kobe, 2008.

21. Bahr, A., J. J. Leonard and A. Martinoli, "Dynamic Positioning of Beacon Vehicles for Cooperative Underwater Navigation", *2012 IEEE/RSJ International Conference on Intelligent Robots and Systems*, pp. 3760–3767, Algarve, 2012.

22. Fan, G., Y. Zhang, Z. Yuan, F. Wang, Y. Li, X. Zhang and J. Li, "Survey of Terrain-Aided Navigation Methods for Underwater Vehicles", *IEEE Access*, Vol. 11, pp. 47510–47526, 2023.

23. Engel, R. and J. Kalwa, "Relative Positioning of Multiple Underwater Vehicles in the GREX project", *Oceans 2009-Europe*, pp. 1–7, 2009.

24. Islam, T. and Y. K. Lee, "A Two-Stage Localization Scheme with Partition Handling for Data Tagging in Underwater Acoustic Sensor Networks", *Sensors*, Vol. 19, No. 9, 2019.

25. Paull, L., S. Saeedi, M. Seto and H. Li, "AUV Navigation and Localization: A Review", *IEEE Journal of Oceanic Engineering*, Vol. 39, No. 1, pp. 131–149, 2014.

26. Auger, F., M. Hilairet, J. M. Guerrero, E. Monmasson, T. Orlowska-Kowalska and S. Katsura, "Industrial Applications of the Kalman Filter: A Review", *IEEE Transactions on Industrial Electronics*, Vol. 60, No. 12, pp. 5458–5471, 2013.

27. Gamse, S., "Dynamic Modelling of Displacements on an Embankment Dam Using the Kalman Filter", *Journal of Spatial Science*, Vol. 63, No. 1, pp. 3–21, 2014.

28. He, B., H. Zhang, C. Li, S. Zhang, Y. Liang and T. Yan, "Autonomous Navigation for Autonomous Underwater Vehicles based on Information Filters and Active Sensing", *Sensors*, Vol. 11, No. 11, pp. 10958–10980, 2011.

29. Prestero, T., *Verification of a Six-Degree of Freedom Simulation Model for the REMUS Autonomous Underwater Vehicle*, M.S. Thesis, Massachusetts Institute of Technology, 2011.

30. Doherty, S. M., *Cross Body Thruster Control and Modeling of a Body of Revolution Autonomous Underwater Vehicle*, M.S. Thesis, Naval Postgraduate School, 2011.

31. Lakhekar, G. and L. Waghmare, "Robust Maneuvering of Autonomous Underwater Vehicle: An Adaptive Fuzzy PI Sliding Mode Control", *Intelligent Service Robotics*, Vol. 10, pp. 195–212, 2017.

32. Navidi, N. and R. Landry, "A New Perspective on Low-Cost MEMS-Based AHRS Determination", *Sensors*, Vol. 21, No. 4, 2021.

33. Sendra, S., J. Lloret, J. M. Jimenez and L. Parra, "Underwater Acoustic Modems", *IEEE Sensors Journal*, Vol. 16, No. 11, pp. 4063–4071, 2016.

APPENDIX A1: SIMULATION COEFFICIENTS

Table A1.1. Force coefficients for REMUS-100 vehicle simulation.

Parameter	**Value**	**Description**
X_{uu}	-1.62	Axial Drag
X_{wq}	$-3.55e+001$	Added Mass
X_{qq}	-1.93	Added Mass
X_{vr}	$3.55e+001$	Added Mass
X_{rr}	-1.93	Added Mass
Y_{vv}	$-1.31e+003$	Cross-Flow Drag
Y_{rr}	$6.32e-001$	Cross-Flow Drag
Y_{uv}	$-2.86e+001$	Body Lift Force
Y_{wp}	$3.55e+001$	Added Mass
Y_{ur}	5.22	Added Mass and Fin Lift
Y_{pq}	1.93	Added Mass
Z_{ww}	$-1.31e+002$	Cross-Flow Drag
Z_{qq}	$-6.32e-001$	Cross-Flow Drag
Z_{uw}	$-2.86e+001$	Body Lift Force
Z_{uq}	5.22	Added Mass and Fin Lift
Z_{vp}	$-3.55e+001$	Added Mass
Z_{rp}	1.93	Added Mass

Table A1.2. Moment coefficients for REMUS-100 vehicle simulation.

Parameter	**Value**	**Description**
K_{pp}	$-1.30e-001$	Rolling Resistance
M_{ww}	3.18	Cross-Flow Drag
M_{qq}	$-1.88e+002$	Cross-Flow Drag
M_{rp}	4.86	Added Mass
M_{uq}	-2	Added Mass and Fin Lift
M_{vp}	-1.93	Added Mass
N_{vv}	-3.18	Cross-Flow Drag
N_{rr}	$-9.40e+001$	Cross-Flow Drag
N_{uv}	$-2.40e+001$	Body Lift and Munk Moment
M_{pq}	-4.86	Added Mass

Table A1.3. Non-linear coefficients for REMUS-100 vehicle simulation.

Parameter	**Value**	**Description**
$M_{\dot{w}}$	-1.93	Added Mass
$M_{\dot{q}}$	-4.88	Added Mass
$N_{\dot{v}}$	1.93	Added Mass
$N_{\dot{r}}$	-4.88	Added Mass
$X_{\dot{u}}$	$-9.30e-001$	Added Mass
$Y_{\dot{v}}$	$-3.55e+001$	Added Mass
$Y_{\dot{r}}$	1.93	Added Mass
$Z_{\dot{w}}$	-4.86	Added Mass
$Z_{\dot{q}}$	-1.93	Added Mass

APPENDIX A2: MATLAB CODE

```
tableData = readtable("accelartionData.xlsx");
time = tableDat.sec; %time
g = 9.81;

%leader and follower accelerations in body-fixed frame
aXFollowerBody = table.aXFollower.*g;
aYFollowerBody = table.aYFollower.*g;
aZFollowerBody = table.aZFollower.*g;

aXLeaderBody = table.aXLeader.*g;
aYLeaderBody = table.aYFollower.*g;
aZLeaderBody = table.aZLeader.*g;

%orientation
for i=1:length(time)
    %follower
    pitchFollower(i) = asin(aXFollowerBody(i)/g);
    rollFollower(i) = atan(aYFollowerBody(i)/aXFollowerBody
       (i));
    %leader
    pitchLeader(i) = asin(aXLeaderBody(i)/g);
    rollLeader(i) = atan(aYLeaderBody(i)/aXLeaderBody(i));
end


%transformation to earth-fixed frame
for i=1:length(time)
    %follower
```

```
rotationFollower = [cos(pitchFollower(i))*cos(
   yawFollower) sin(rollFollower(i))*sin(pitchFollower(
   i))*cos(yawFollower)-cos(rollFollower(i))*sin(
   yawFollower) sin(yawFollower)*sin(rollFollower(i))+
   cos(yawFollower)*sin(pitchFollower(i))*cos(
   rollFollower(i)); ...
                  cos(pitchFollower(i))*sin(
                     yawFollower) sin(yawFollower)*sin
                     (pitchFollower(i))*sin(
                     rollFollower(i))+cos(yawFollower)
                     *cos(rollFollower(i)) cos(
                     rollFollower(i))*sin(
                     pitchFollower(i))*sin(yawFollower
                     )-sin(rollFollower(i))*cos(
                     yawFollower); ...
                  -sin(pitchFollower(i)) sin(
                     rollFollower(i))*cos(
                     pitchFollower(i)) cos(
                     pitchFollower(i))*cos(
                     rollFollower(i))];
aFollower(:,i) = rotationFollower*[aXFollowerBody(i);
   aYFollowerBody(i);aZFollowerBody(i)];
%leader
YonelimMatrisi2 = [cos(pitchLeader(i))*cos(yawLeader)
   sin(rollLeader(i))*sin(pitchLeader(i))*cos(yawLeader
   )-cos(rollLeader(i))*sin(yawLeader) sin(yawLeader)*
   sin(rollLeader(i))+cos(yawLeader)*sin(pitchLeader(i)
   )*cos(rollLeader(i)); ...
                  cos(pitchLeader(i))*sin(yawLeader)
                     sin(yawLeader)*sin(pitchLeader(i)
                     )*sin(rollLeader(i))+cos(
```

```
                        yawLeader)*cos(rollLeader(i)) cos
                        (rollLeader(i))*sin(pitchLeader(i
                        ))*sin(yawLeader)-sin(rollLeader(
                        i))*cos(yawLeader); ...
                    -sin(pitchLeader(i)) sin(rollLeader(
                        i))*cos(pitchLeader(i)) cos(
                        pitchLeader(i))*cos(rollLeader(i)
                        )];
    aLeader(:,i) = rotationFollower*[aXLeaderBody(i);
       aYLeaderBody(i);aZLeaderBody(i)];
end


%dead reckoning navigation
for i=2:length(time)
    %Follower
    vFollower(i) = vFollower(i-1) + aFollower(i-1).*dt;
    xFollower(i) = xFollower(i-1) + vFollower(i-1).*dt;
    %Leader
    vLeader(i) = vLeader(i-1) + aLeader(i-1).*dt;
    xLeader(i) = xLeader(i-1) + vLeader(i-1).*dt;
end

%relative navigation
for i=2:length(time)
    xEstimateHat = A*xEstimate(:,i-1);
    P = A*P*A' + xEstimateHat;
    %Kalman Gain
    K = P*H'/(H*P*H'+R);
    %Measure
    yMeasurement = [xSonar(i) vXSonar(i) aFollower(1,i)-
```

```
        aLeader(1,i)...
                        ySonar(i) vYSonar(i) aFollower(2,i)-
                            aLeader(2,i)]';
    %Update
    xEstimate(:,i) = xEstimateHat + K*(yMeasurement-H*
        xEstimateHat);
    P = (eye(6)-K*H)*P;
end
```